DEVELOPMENT OF A SHORT PULSED SOLID PROPELLANT PLASMA THRUSTER

FINAL REPORT
FAIRCHILD REPUBLIC COMPANY
MS172R0001

William J. Guman

10 March 1974
Contract No. NAS1-11812
Contract No. 953656

This work was performed for the Jet Propulsion Laboratory, California Institute of Technology sponsored by the National Aeronautics and Space Administration under Contract NAS7-100.

FAIRCHILD

Fairchild Republic Company Farmingdale, L.I. New York 11735

Prepared for
Jet Propulsion Laboratory
California Institute of Technology
Pasadena, California

DEVELOPMENT OF A SHORT PULSED SOLID PROPELLANT PLASMA THRUSTER

FINAL REPORT
FAIRCHILD REPUBLIC COMPANY
MS172R0001

William J. Guman

10 March 1974
Contract No. NAS1-11812
Contract No. 953656

This work was performed for the Jet Propulsion Laboratory, California Institute of Technology sponsored by the National Aeronautics and Space Administration under Contract NAS7-100.

FAIRCHILD

Fairchild Republic Company Farmingdale, L.I. New York 11735

Prepared for
Jet Propulsion Laboratory
California Institute of Technology
Pasadena, California

ACKNOWLEDGEMENT

The author would like to acknowledge the invaluable contributions of Mr. M. Katchmar in carrying out the studies. The assistance of Mr. J. McIver in carrying out the electrostatic augmentation studies is also gratefully acknowledged as well as the stimulating discussions with Dr. D. Palumbo. Dr. Vondra of MIT Lincoln Laboratory most kindly provided on a loan basis a bank of three capacitors which enabled the capacitor studies to be carried out after numerous failures had been encountered. The technical effort was initially carried out under the technical direction and guidance of Messrs. J. Hoell and E. Van Landingham of NASA Langley and subsequently by Messrs. J. Dahlgren and G. Hotz of the Jet Propulsion Laboratory of the California Institute of Technology. The latest efforts were under the technical direction of Mr. D. Fitzgerald of the Jet Propulsion Laboratory.

TABLE OF CONTENTS

Paragraph			Page
1.0	INTRODUCTION		1
	1.1	Background	1
2.0	SINGLE TURN OPEN LOOP SOLID PROPELLANT FEED SYSTEM		2
	2.1	Design Considerations	2
	2.2	Experimental Verification	5
3.0	HIGH ENERGY DENSITY ENERGY STORAGE CAPACITOR EVALUATION STUDIES		12
	3.1	Capacitor Evaluation in a Vacuum Environment	12
	3.2	Thermal-Vacuum Test	19
	3.3	Prolonged Operation in a Vacuum	30
	3.4	Conclusions and Recommendations	34
4.0	ELECTROSTATIC AUGMENTATION STUDIES		35
	4.1	Background	35
	4.2	Effect of the Direction of the Electric Field (Electrode Polarity)	42
	4.3	Effect of Amplitude of the Self Applied Field	47
	4.4	Effect of an Auxiliary Electric Field	48
	4.5	Concluding Remarks	55
5.0	REFERENCES		56

LIST OF FIGURES

Figure		Page
1	Circular Propellant Feed System Microthruster	4
2	Rear View of Spring Feed System Microthruster	6
3	Circular Propellant Rod after 7,909,297 Discharges	8
4	Capacitor-Thruster Test Assembly	15
5	Front View of Capacitor-Thruster Test Assembly	16
6	Radiation Cooled Thermal-Vacuum Temperature History (73.77 watts)	21
7	Radiation Cooled Thermal-Vacuum Temperature History (97.00 watts)	22
8	Radiation Cooled Thermal-Vacuum Temperature History (133.8 watts)	23
9	Conduction Cooled Thermal-Vacuum Temperature History (75.4 watts)	24
10	Conduction Cooled Thermal-Vacuum Temperature History (98.9 watts)	25
11	Conduction Cooled Thermal-Vacuum Temperature History (129.2)	26
12	Equilibrium Temperature as a Function of Input Power	29
13	Details of Conical Nozzle Design	37
14	Front View of Conical Nozzle Thruster	38
15	Rear View of Conical Nozzle Thruster	39
16	Location of Electrodes During Field Direction Tests	42
17	Modified Thruster with Upstream Located Igniter Plug	44
18	Conical Nozzle with Upstream Located Igniter Plug	45

LIST OF FIGURES (Continued)

Figure		Page
19	Block Diagram of Equipment Used for Externally Applied Electrostatic Field Experiments	49
20	Sketch of Vacuum Switch Integrated to Thruster	41
21	Discharge Behavior of External Field Circuit and Main Thruster Discharges	54

LIST OF TABLES

Table		Page
1	Total Impulse Requirements for N-S Station Keeping	2
2	Number of Turns in Helical Propellant Coil	3
3	Measured Performance of Circular Propellant Feed System Microthruster	5
4	Test Results of Circular Feed System	7
5	Propellant System Test Data	9
6	Thermocouple Location	17
7	Conditions of Radiation Cooled Thermal-Vacuum Test	17
8	Temperature Data of Tests	18
9	CSI Capacitor Data	18
10	Summary of Test Results (Equilibrium Temperature)	27
11	Peak Discharge Current Data	28
12	Temperature Data During Vacuum Life Test	31
13	Pulse Frequency Checks	33
14	Peak Discharge Current Amplitude Checks	33
15	Total Shots as Each of Three MIT L/L Provided High Energy Density Capacitors	33
16	Experimental Results (Log 151-1) Conical Thruster-Cathode Downstream	40
17	Polarity Effect on Performance	41
18	Polarity Test Results	46
19	Comparison of Test Results	46
20	Electric Field Strength Tests	47
21	Correlations Observed	48
22	Performance Measurement with and without Externally Applied Electrostatic Field	53

ABSTRACT

This report summarizes the experimental results that were obtained in the development of a Teflon solid propellant pulsed plasma thruster. Three studies were performed. One of the studies established the feasibility of storing and feeding solid propellant in the form of an open circular loop into an operational thruster. This technique was verified to be practical by feeding over 20 inches of Teflon into a micro-thruster over an accumulated life test of 1858 hours. The second study evaluated high energy density capacitors under vacuum conditions when the capacitor is coupled directly to a plasma thruster. Numerous early capacitor failures were encountered. Evidence leads one to conclude that essentially all of the failures encountered in a vacuum environment are due to an internal electrical breakdown that will occur inside a capacitor that is not truly hermetically sealed. A bank of three hermetically sealed capacitors rated at 16.4 joules/lb. (7.45 joules/Kg) was thermal vacuum and life tested. Under radiation cooled conditions, the capacitor bank could safely tolerate 130 watts of input power steadily when radiating to a 27.2°C sink. A steady input power significantly in excess of 130 watts can safely be tolerated if heat conduction can be provided to a sink whose temperature is about 16°C. A vacuum life test of the capacitor bank was carried out while discharging into a milli-lb. (milli-Newton) type pulsed plasma thruster. The test was carried out at an input power level of about 110 watts under radiation cooled conditions. More than 1500 hours of vacuum testing of this milli-pound (milli-Newton) type system has been accumulated up to the end of the program without any capacitor problems. Recommendations are made for future capacitor designs. The third set of studies examined electrostatic field effects on thruster performance in a conical electrode geometry. It was deduced that due to the low specific impulse encountered with this new geometry, no definite conclusions could yet be made and that future testing must be carried out at a higher specific impulse level.

1. INTRODUCTION

1.1 BRIEF BACKGROUND

The feasibility of the solid propellant pulsed plasma microthruster as a reliable space propulsion system was verified during 5 years of space flight aboard the LES-6 satellite. More than 8900 hours of operation was demonstrated at synchronous altitude. The ability to scale the solid propellant microthruster concept into the milli-lb (milli-Newton) regime was subsequently demonstrated [1, 2, 3]. These latter studies were carried out with laboratory type hardware and clearly revealed the need for further developmental studies of solid propellant feed systems compatible with large total impulse missions and also the necessity of developing high energy density capacitors capable of operating reliably in a vacuum environment. This report summarizes the developmental studies in these two latter areas of endeavor as well as the studies that were performed in an attempt to improve propulsive performance by utilizing electrostatic field efforts in a conically shaped electrode nozzle geometry.

2. SINGLE TURN OPEN LOOP SOLID PROPELLANT FEED SYSTEM

2.1 DESIGN CONSIDERATIONS

It has generally been believed that the solid propellant thruster represents an impractical system for large total impulse missions because the solid propellant rod of solid propellant plasma thrusters has previously been stored in the form of a straight rod in microthrusters. Some simple calculations were presented [4] to disprove such a belief. Suppose one briefly reviews some of the calculations in conjunction with experimental data [1] that was demonstrated prior to the program being reported upon.

In Reference 4 it was recommended that the solid propellant for large total impulse missions be stored in the form of a helical coil with the thruster capacitor and system electronics stored within the coil in order to minimize the volume of the total system. Assuming a ΔV for North-South station keeping of 170 ft/sec-year, Table 1 presents the total impulse requirements of a 1000, 2000 and 3000 lb. satellite for a 1, 5, 7, and 10 year mission.

The impulse to be provided about the nodal points is produced by a pair of thrusters, each carrying propellant to provide half the total impulse shown in Table 1. With the propellant of each thruster stored in the form of a 12-inch (30.5 cm) diameter helical coil and having a frontal area of 2.93 in.^{2} (18.9 cm^2) the number of turns in the coil required to provide the total impulse are presented in Table 1. The calculations are based upon a specific impulse of 1900 sec, a value experimentally demonstrated in an earlier program with a propellant having a frontal area of 2.93 in.^{2} (18.9 cm^2).

TABLE 1. TOTAL IMPULSE REQUIREMENTS FOR N-S STATIONKEEPING

ΔV = 170 ft/sec-year

Satellite Weight (lb)	1 Year	5 Years	7 Years	10 Years
1000	5,270	26,400	36,900	52,700
2000	10,540	52,800	73,600	105,400
3000	15,810	79,200	110,500	158,100

The results presented in Table 2 show that the number of turns required to store large quantities of solid propellant are so small that a simple spring feed system can be used even for the 10 year total impulse requirements of a 3000 lb. (1360 Kg) satellite.

TABLE 2. NUMBER OF TURNS IN HELICAL PROPELLANT COIL
(Specific Impulse 1900 sec, Propellant Area 18.9 cm^2)

Satellite Weight (lb)	3 Years	5 Years	7 Years	10 Years
1000	0.493	0.82	1.15	1.64
2000	0.986	1.64	2.30	3.28
3000	1.479	2.46	3.45	4.42

From the results of the simple calculations presented it can be seen that if the solid propellant were stored in the form of a spring fed circular loop (i.e., a single turn of solid propellant), sufficient propellant could even then be stored for missions requiring as much as 20,000 lb-sec (88,964 N-sec) of total impulse per thruster. Because of the very low vapor pressure of Teflon, the Teflon-spring feed assembly can be stored directly in a vacuum with a minimum of structural support.

The design and test of an experimental solid propellant feed system consisting of a spring fed circular, single turn open loop of propellant was carried out under Program NAS 1-11812.

To facilitiate a laboratory evaluation of the circular propellant feed system under actual thruster operating conditions and within available program time, a "microthruster" was designed to operate at a relatively low specific impulse (below 1000 seconds) in order to test the propellant system.

The Teflon propellant rod of the circular feed system was turned on a lathe from a solid slab of Teflon. The Teflon was purchased in a stress relieved form. No problems were encountered in fabricating the circular open loop of Teflon even though it was required that its OD be $10.000\ ^{+0.005}_{-0.000}$ inches and its ID $8.440\ ^{+0.005}_{-0.000}$ inches. The ability to machine the Teflon to these tolerances was of some concern. However it was found that a completely stress relieved piece of Teflon presents no problem in being fabricated to the desired shape. Figure 1 shows a side view of

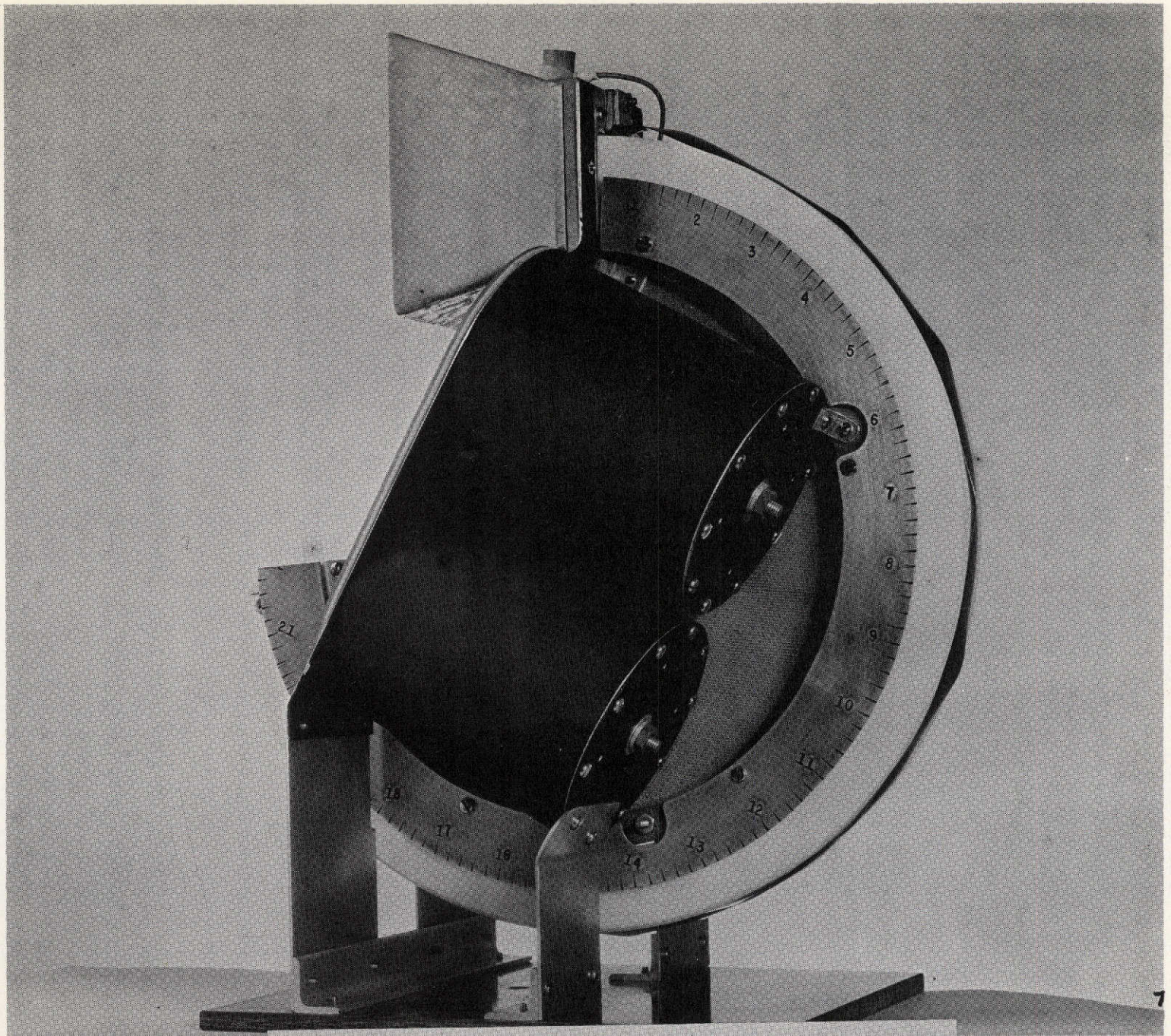

Figure 1. Circular Propellant Feed System Microthruster

this propellant system as part of a microthruster. It is seen that about 22 inches (55.8 cm) of propellant can indeed be stored in a minimum volumetric configuration. The single Negator spring is located in a very simple manner on the outside of the loop of the solid propellant as can be seen in Figure 2.

2.2 EXPERIMENTAL VERIFICATION

The microthruster with the circular solid propellant feed system was placed on a direct thrust measuring balance in a vacuum chamber and tested. Table 3 presents the performance results that were measured.

TABLE 3. MEASURED PERFORMANCE OF CIRCULAR PROPELLANT FEED SYSTEM MICROTHRUSTER

Thrust Level:	177.6 micro-lb (790.3 micro-Newtons)
Impulse Bit Amplitude:	97.58 micro-lb-sec (434.2 micro-Newton - sec)
Pulse Frequency:	1.82 Hz
Discharge Energy:	16.8 joules
Thrust/Power Ratio:	5.81 micro-lb/watt (25.84 micro-Newton/watts)
Power/Thrust Ratio:	172.1 watts/mlb (38.69 watts/milli-Newton)

Even though this microthruster was designed and assembled only for the purpose of testing the circular propellant feed concept it can be seen that its performance as a microthruster is still attractive for microthruster applications.

Uninterrupted vacuum testing of the circular propellant feed system was carried out. The spring fed circular propellant was fed into the thruster as simply as one feeds a straight rod and it was verified that this concept of storing solid propellant represents a practical concept that can be used any time where such an approach would be desirable to minimize total system geometry or where solid propellant for a total impulse of perhaps as much as 20,000 lb-sec (88,964 N-sec) per nozzle is desired. After 7,909,297 discharges some intermittency in thruster operation occurred. At this time 13.3 inches (33.8 cm) of teflon had been used (165° of propellant movement). Since the propellant feed test was flawless up to this

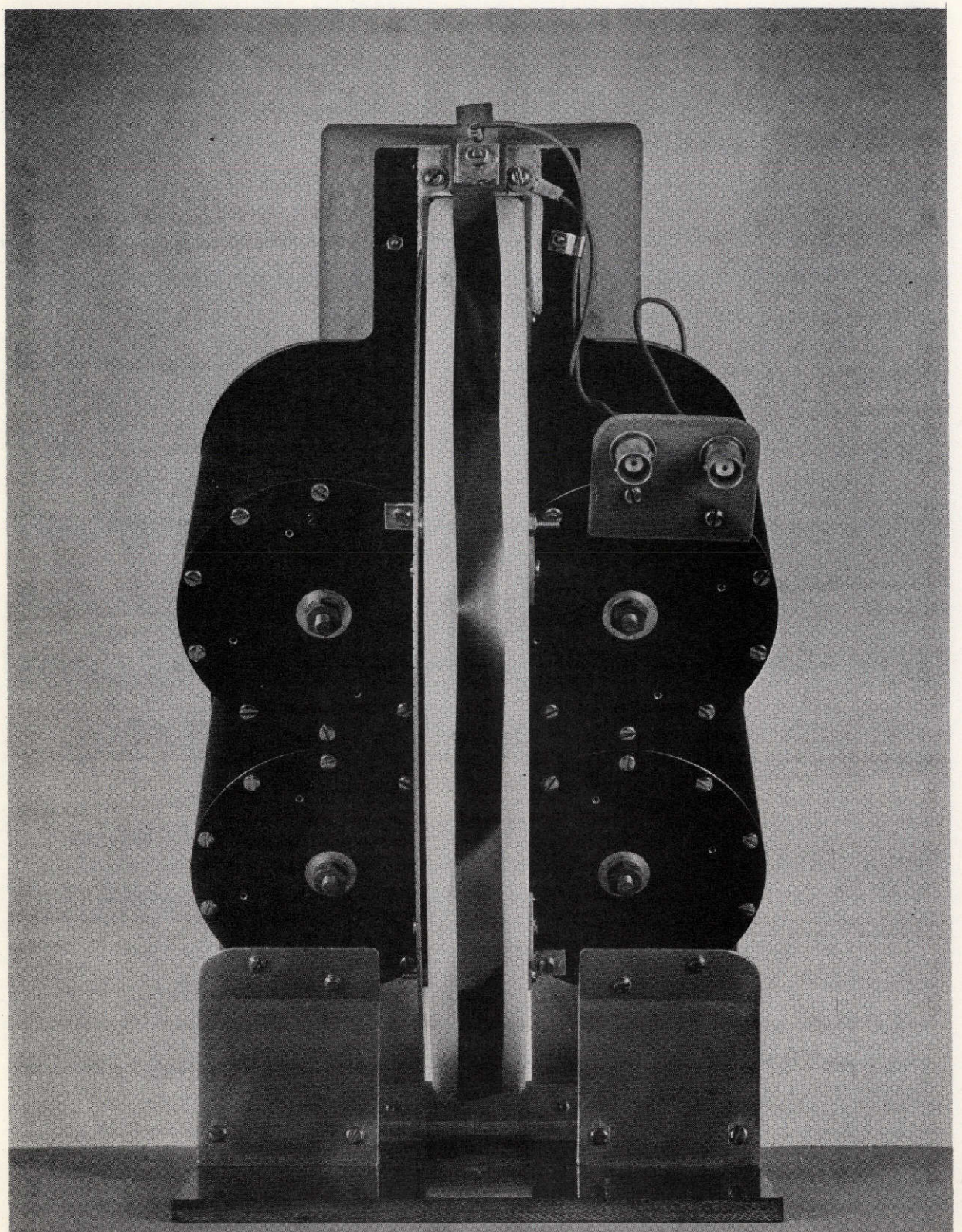

Figure 2. Rear View of Spring Feed System Microthruster

point, it was decided to interrupt the propellant feed test in order to determine the reason for intermittency in thruster operation. With the thruster high voltage removed it was found that igniter plug discharges were intermittent thus pinpointing thruster intermittency to the igniter plug. The plug was cleaned and once more it operated normally. It was concluded that deposits which formed on the igniter plug partially covered the semiconductor of the igniter plug and prevented it from igniting the main discharge. A modification of the ignition system was made and testing of the propellant system was resumed.

Figure 3 shows the system after it was removed from the vacuum chamber. This Figure should be compared with Figure 1 which shows the propellant rod prior to testing. Figure 3 shows the solid propellant rod at the new peripheral location of 8.35 inches (2.12 cm), i.e., after 165° of propellant consumption. Roughly 800 lb-sec (3558 Newton-sec) of total impulse were generated by the microthruster system before the test was interrupted to clean the igniter plug.

Table 5 presents a summary of the test data of the uninterrupted test of the circular propellant system. Propellant consumption was quite consistent throughout the test thereby verifying that propellant binding or hangup does not occur as Holcomb [5] thought might occur.

Testing of the circular feed propellant system was resumed until all of the available solid propellant was consumed. Two additional interruptions were made because of minor problems with the ignition system. The status of the propellant at the time the interruptions were made is presented in Table 4.

TABLE 4. TEST RESULTS OF CIRCULAR FEED SYSTEM

Discharges	Length of Propellant Used	Arc Length Used	Log
0 - 1,048,020	System Checkout	--	148-1, 2
1,048,020 - 7,909,297	13.30 inches (33.78 cm)	165°	148-3
7,909,297 - 9,736,781	16.54 inches (42.01 cm)	205°	148-4
9,737,208 - 10,357,287	17.52 inches (44.50 cm)	217°	148-5
10,357,406 - 12,244,285	20.42 inches (51.87 cm)	253°	148-6

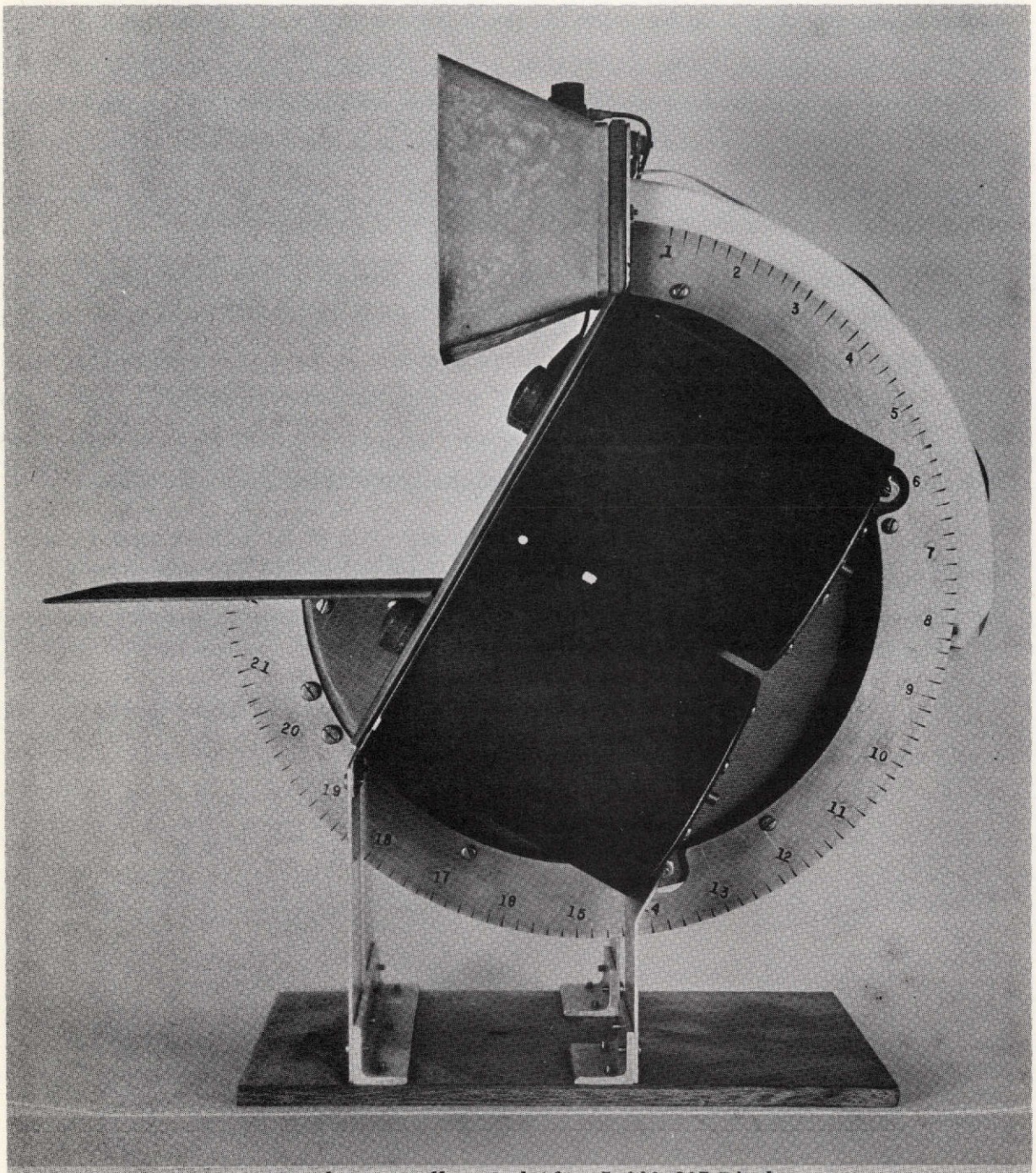

Figure 3. Circular Propellant Rod After 7,909,297 Discharges

TABLE 5. PROPELLANT SYSTEM TEST DATA

Date (1972)	Count	Daily or Weekend Shots	Fuel Ind. (in.)	Week End or Daily Used (in.)	Total Used (in.)	Total Used (cm)
Sept 22	43,961		21.65	0	0	0
25	464,455	420,494	20.87	.78	.78	1.98
26	619,400	154,945	20.58	.29	1.07	2.72
27	772,890	153,490	20.31	.27	1.34	3.40
28	926,550	153,660	20.03	.28	1.62	4.11
29	1,048,020	121,470	19.85	.18	1.80	4.57
Oct 3	1,196,840	148,820	19.60	.25	2.05	5.21
4	1,350,760	153,920	19.32	.28	2.33	5.92
5	1,462,535	111,775	19.14	.18	2.51	6.37
6	1,616,480	153,945	18.87	.27	2.78	7.06
9	2,080,210	463,730	18.12	.75	3.53	8.97
10	2,234,800	154,590	17.90	.22	3.75	9.53
11	2,388,695	153,895	17.65	.25	4.00	10.16
12	2,541,688	152,993	17.40	.25	4.25	10.79
13	2,694,375	152,687	17.15	.25	4.50	11.43
16	3,158,920	464,545	16.38	.77	5.27	13.39
16	3,212,574	53,654	16.30	.08	5.35	13.59
18	3,365,430	152,856	16.07	.23	5.58	14.17
19	3,523,670	158,190	15.83	.24	5.82	14.78
20	3,680,570	156,950	15.56	.27	6.09	15.47
23	4,152,548	471,978	14.75	.81	6.90	17.53

TABLE 5. PROPELLANT SYSTEM TEST DATA (Continued)

Date (1972)	Count	Daily or Weekend Shots	Fuel Ind. (in.)	Week End or Daily Used (in.)	Total Used (in.)	Total Used (cm)
Oct 24	4,309,930	157,382	14.50	.25	7.15	18.16
25	4,467,000	157,070	14.25	.25	7.40	18.79
26	4,624,000	157,000	13.98	.27	7.67	19.48
27	4,774,730	150,730	13.73	.25	7.92	20.12
30	5,232,275	471,545	12.92	.81	8.73	22.17
30	5,409,330	157,055	12.67	.25	8.98	22.87
Nov 1	5,566,130	156,800	12.40	.27	9.25	23.49
2	5,722,450	156,320	12.13	.27	9.52	24.18
3	5,878,400	155,950	11.87	.27	9.79	24.87
6	6,349,550	471,150	11.03	.83	10.62	26.97
8	6,663,250	313,700	10.50	.53	11.15	28.32
9	6,816,600	153,350	10.24	.26	11.41	28.98
10	6,972,500	155,900	9.97	.27	11.68	29.67
13	7,443,820	471,320	9.17	.80	12.48	31.70
14	7,600,750	156,930	8.88	.29	12.77	32.44
15	7,756,950	156,200	8.61	.27	13.04	33.12
16	7,903,195	146,245	8.35	.26	13.30	33.78

A total of 12,244,285 discharges were delivered with 20.42 inches (51.87 cm) of solid Teflon consumed. The measured weight change was 862.2756 grams. At no time during the entire circular feed test duration of an accumulated 1858 hours was any problem encountered with the circular feed system. The problem with the igniter plug encountered after 1200 hours of uninterrupted system operation is independent of the feed system. Thus it can be concluded that the technique of storing propellant in the form of a single turn open loop of solid propellant and feeding it with a simple Negator spring has been verified to be a practical concept.

3. HIGH ENERGY DENSITY ENERGY STORAGE CAPACITOR EVALUATION STUDIES

3.1 CAPACITOR EVALUATION IN A VACUUM ENVIRONMENT

During Contract NAS1-10944 two energy storage capacitors (Model 3E014) comprised of a Kaptan dielectric system were built by CSI and laboratory tested at Fairchild Republic. These capacitors were tested at an energy/weight ratio of about 10 joules/lb. Both of these capacitors failed almost immediately after they were placed on test [2]. Near the end of that program they were returned to the vendor for failure analysis and repair. The vendor repaired both units and they were returned to Fairchild Republic for retesting under the present program. The vendor stated that the dielectric film (Kaptan) originated from a poor manufacturer's lot and that the repaired units were again fabricated with more care from the same lot of material.

The repaired Model 3E014 capacitor was placed in a vacuum chamber and retested. The capacitor failed again after only 5 discharges. The failure once more appeared as a short with a resistance of 1 ohm between terminals. The thruster nozzle assembly was removed and placed on the second repaired capacitor. This unit also failed after only 395 discharges. The failure again appeared as a short with a resistance of 1.5 ohms between terminals.

Two entirely new capacitors (Models 3W355 and 3W356) built by CSI utilizing a new superior construction technique were obtained as GFE for evaluation. Thermocouples were provided on the side of one of the capacitors and also on the thruster strip line connecting the capacitor to the thruster nozzle. A Rogowsky coil was also located in the discharge circuit to record the discharge current. On raising the applied voltage from zero volts slowly to the design voltage of 3 KV while the capacitor was in a vacuum, a failure occurred at about 2.2 KV with only 14 discharges on the capacitor. The failure appeared as a short with a resistance of about 0.1 ohms between terminals. CSI was informed of this failure. The Model 3W355 capacitor was shipped back to the vendor for a failure analysis.

Upon inspection of the failed unit, the vendor suggested that the capacitor had failed under an over-voltage condition. Since the capacitor was tested under room conditions at CSI, an over-voltage condition would have been required for the observed failure-producing type of flashover to occur under atmospheric conditions.

However, when the pressure is locally reduced below atmospheric pressure, such as occurs during thruster operation, the same type of flashover can occur at much lower test voltages. This latter discharge behavior is commonly described by a Paschen curve. Since the failed capacitor was subjected at Fairchild Republic to a 16-day vacuum soak of about 1.7×10^{-5} mm Hg at room temperature, it appears that a reduced pressure environment developed inside the capacitor during this vacuum soak. When the capacitor was subsequently electrically charged during testing, a Paschen type breakdown occurred inside the capacitor. Fairchild Republic informed CSI of the proposed failure mechanism and CSI considered techniques for eliminating such a failure mode in future designs. The second GFE capacitor, a 500 joule unit (Model 3W356) was returned to CSI without having been electrically tested at Fairchild Republic.

It is understood that the two capacitors were subsequently modified by CSI to have the liquid impregnant inside the capacitor under a positive pressure at room temperature. This technique is to preclude the possibility of a void from forming inside the capacitor. Upon receiving the improved versions, the 500 joule capacitor (Model 3W356) was prepared for a thermal vacuum test. Thermocouples were provided at the following locations:

1) Directly under the cathode of the thruster nozzle
2) On the center of the negative strip line between the capacitor and the cathode
3) Under the nut of one of the negative terminals at the capacitor
4) On the side surface of the capacitor

The first thermal vacuum test was to be performed under radiation cooled conditions at a 100 watt power level (a 500 joule discharge once every 5 seconds). The test was started but had to be terminated after 8 discharges due to a capacitor failure.

Since a small K-film capacitor (Model 2K126, 10 mfd 2 KV) of CSI was available, it was decided to evaluate this unit also. After 513 discharges this capacitor failed also.

Due to the poor performance of the various CSI capacitors tested, it was decided not to retest the repaired Model 3W555 capacitor.

In a subsequent discussion with Mr. Hayworth, President of CSI, it was learned that all of the CSI capacitors which failed at Republic (Kapton, Mylar, K-film) were of a multi-pad construction. Mr. Hayworth believed that this type of construction may be susceptible to a voltage multiplication due to internal electric wave interactions. Since single pad type of Mylar capacitors built at CSI under the supervision of MIT Lincoln Laboratory had not failed either at MIT Lincoln Laboratory or at Fairchild Republic, Republic was advised that they would receive four MIT type capacitors built by CSI for evaluation. These latter type of Mylar-Aerochlor capacitor when evaluated at 3 KV would provide discharges at about 16 to 17 joules/lb.

In order to evaluate these new Mylar capacitors, it was necessary to design, fabricate and assemble a new capacitor - thruster nozzle test assembly. The design was performed to accommodate the installation of three of the new type of capacitors. The final test assembly is presented as Figures 4 and 5. When operated at a discharge voltage of 3000 volts, approximately 220 joules of energy would be discharged by the three capacitors into the thruster nozzle load. While the system could not be tested on a thrust balance, each thruster discharge is believed to provide an impulse bit of roughly one milli-lb second at a specific impulse in the neighborhood of 1500 sec.*

Four capacitors built substantially the same as those built under MIT Lincoln Laboratory supervision were received from the vendor. Table 9 presents information regarding these capacitors. Unit K4 was noted to have oil around the high voltage stud when it was received. Since the bushing assemblies varied between the four units, some minor rework of these was required before they could be used in the new thruster test unit. Mr. Hayworth of CSI advised that it was possible to develop a small oil leak in refurbishing the bushing assembly. Indeed, capacitor K3 did develop a leak. All units were subsequently epoxy potted around the bushing assembly to preclude any possible loss of dielectric impregnant during vacuum testing. Units K1, K2 and K4 were installed in the thruster-capacitor test rig in order to perform the required thermal vacuum test. Seven thermocouples were provided to the test assembly to obtain as complete a temperature history as possible. Table 6 presents the location of the thermocouples.

---

* Post program measurements revealed that actually 1.15 millipound-sec impulse bits at a specific impulse of 1780 seconds were produced.

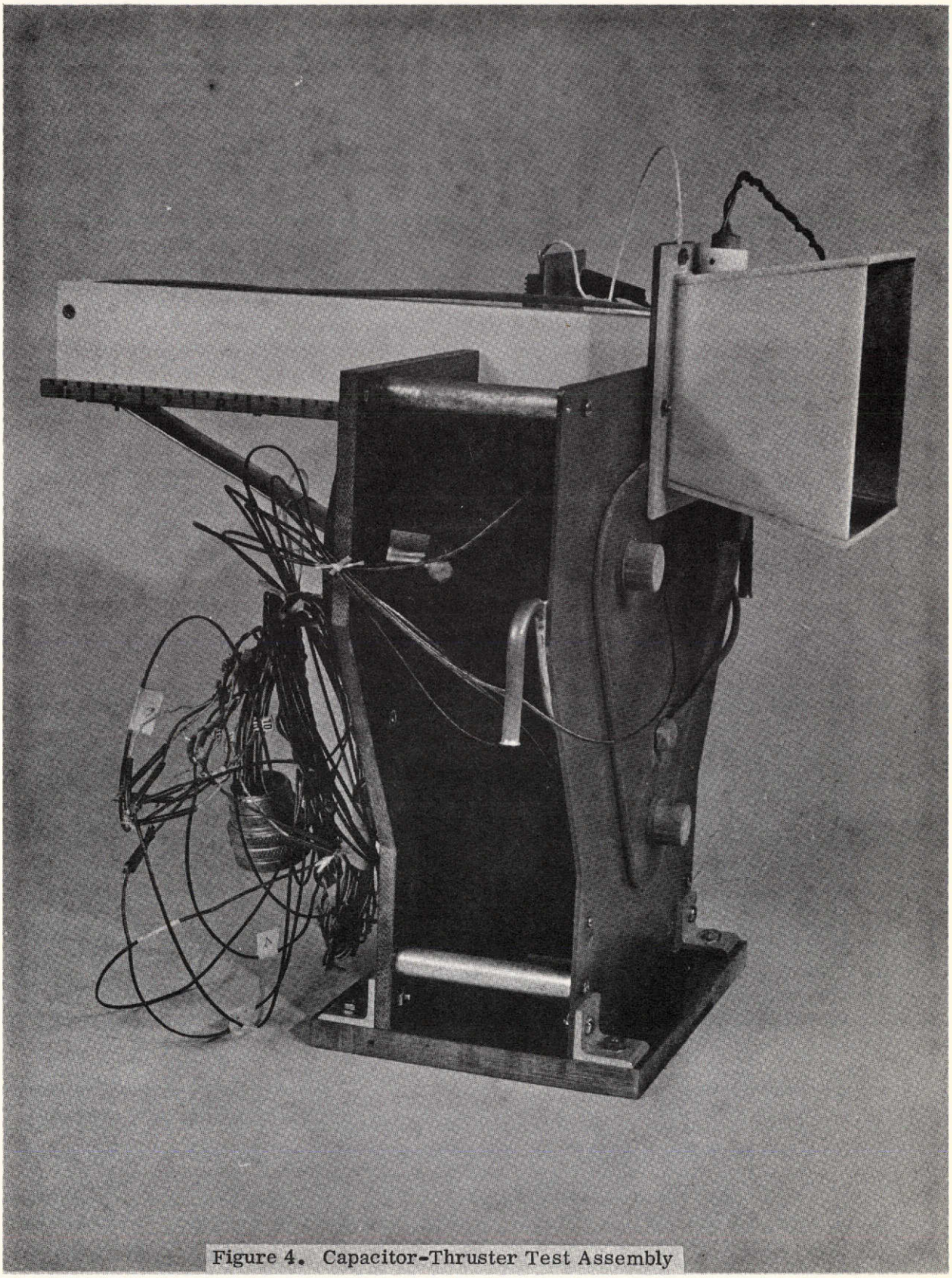

Figure 4. Capacitor-Thruster Test Assembly

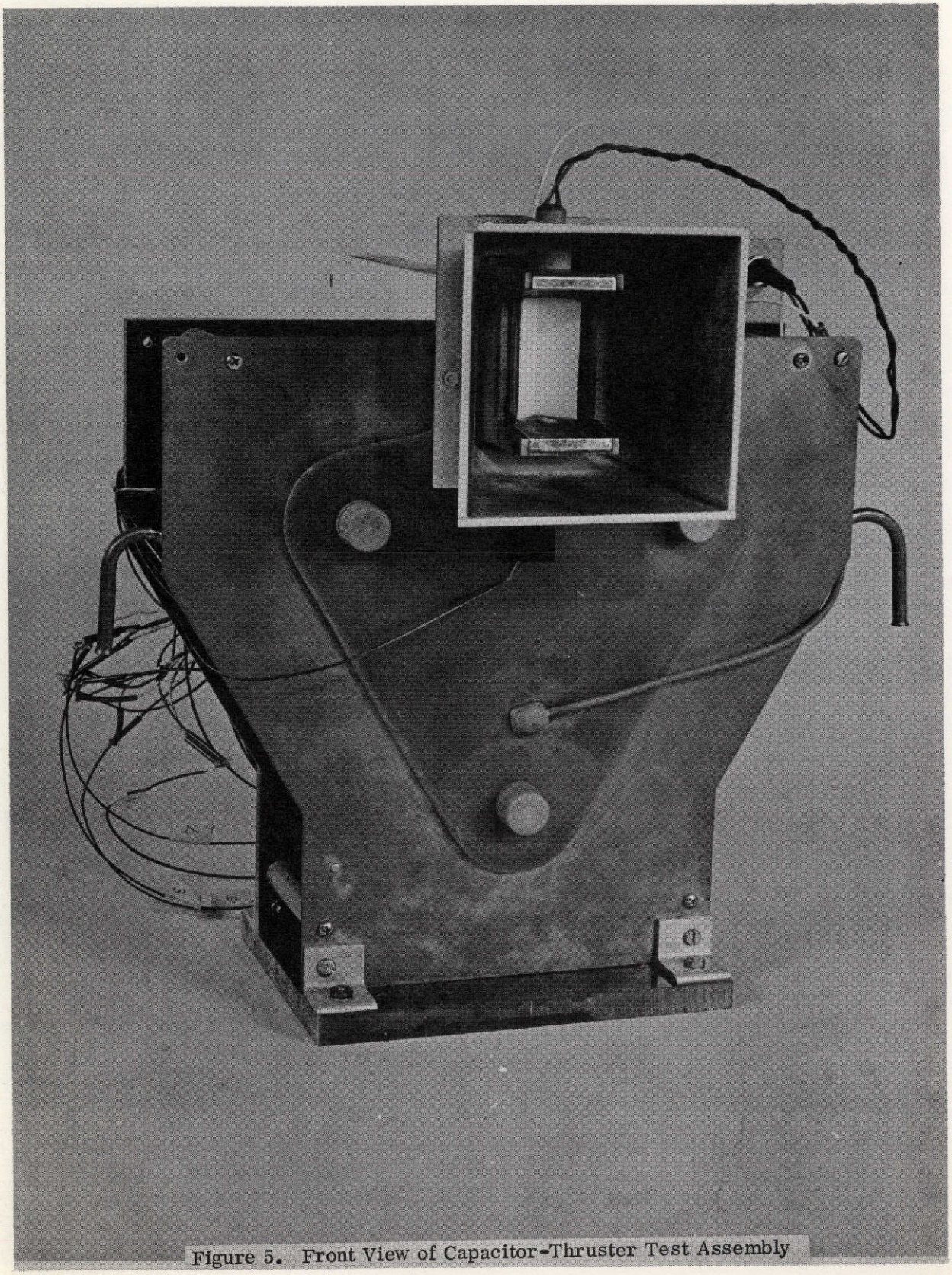

Figure 5. Front View of Capacitor-Thruster Test Assembly

TABLE 6. THERMOCOUPLE LOCATION

Thermocouple No.	Location
1	On the negative strip line at the center of all three capacitors
2	Near the outer edge of the cathode strip line
3	Adjacent to the ground ring on capacitor #1
4	Adjacent to the ground ring on capacitor #2
5	Adjacent to the ground ring on capacitor #3
6	On the cylindrical side of capacitor #1
7	About 1 inch below the anode on the positive strip line

Figure 4 shows the assembled system including the thermocouples and the output lead of the Rogowski coil. A Tektronix high voltage probe was used to present the discharge voltage on an oscilloscope.

The system was mounted in a 6' x 8' vacuum test chamber and prepared for radiation cooled thermal-vacuum tests. The first test was initiated with test conditions presented in Table 7.

TABLE 7. CONDITIONS OF RADIATION COOLED THERMAL-VACUUM TEST

Total Capacitance	48.5 μfd
Test Voltage	2905 volts
Pulse Frequency	0.691 Hz
Discharge Energy	204.6 joules
Power of Operation	141.4 watts

Temperature readings were taken until multi-firing (i.e., misfiring) of the thruster was observed after only 590 discharges had been produced. The thermal-vacuum test had to be interrupted and an attempt was made to isolate the source of

multi-firing. After 1036 discharges the test was terminated and upon opening the vacuum chamber it was found that the cause of thruster multi-firing was another leaky capacitor. The liquid impregnant leaked around the center stud and its vapor pressure prevented system operation in a vacuum. It is interesting to note that this was capacitor K1 (capacitors K3 and K4 had leaked previously). Since it was not possible to carry out the program with the available capacitors, all work had to be stopped on the program. Table 8 presents the limited amount of temperature data that was obtained and Table 9 presents a summary of all of the test results of CSI capacitors that were tested during a 3-year testing period.

TABLE 8. TEMPERATURE DATA OF TESTS (°C)

Pulse Count	1	2	3	4	5	6	7
0	25.0°C	25.0°C	25.0°C	25.0°C	25.0°C	25.0°C	25.0°C
232	26.1	26.1	26.7	26.1	26.1	26.1	33.9
442	28.3	27.8	28.9	28.9	28.3	27.2	45.6

TABLE 9. CSI CAPACITOR DATA

Model	Serial No.	Discharges Before Failure	Failure Mode
3E014		52	short, 40 ohms
3E014		4436	short, 2 ohms
3E014	2598	5	short, 1 ohm
3E014	2727	395	short, 1.5 ohms
3W355	7322	14	short, 0.1 ohm
3W356	(repaired unit)	8	short
2K126		513	short
5W364(K1)		1036	Stud bent, ceramic recessed, leaked under test
5W364(K2)			Capacitor still functional
5W364(K3)		-	Oil leak developed during handling
5W364(K4)			Oil around stud when received

The limited amount of thermal data that was obtained shows that the highest temperature was obtained on the positive strip line below the anode. This latter thermocouple can be seen as the single thin lead on the front face of the thruster assembly (see Figure 5).

Since CSI uses high voltage bushing assemblies from either Alberox or Ceramaseal, the Alberox Company was contacted regarding the dielectric fluid leakage problem encountered with the CSI capacitors. At a meeting at Fairchild Republic, it was learned from Alberox that both Alberox or Ceramaseal can provide helium leak tested bushing assemblies. Capacitor manufacturers such as CSI have the option to purchase either assembled leak tested bushing assemblies or bushings without the center stud or bushings brazed to the capacitor can. It was learned from Mr. White of CSI that because of different customer requirements, CSI elects to buy bushings which are not assembled and leak tested. It would appear that most of the problems encountered with CSI capacitors could evidently be resolved if they were to use capacitor cans with helium leak tested bushing assemblies furnished by either Ceramaseal or Alberox. This conclusion is further substantiated by the fact that capacitor can assemblies sent to CSI by MIT Lincoln Laboratory were provided to CSI in this manner and that no failures of such capacitors were encountered at Republic.

3.2 THERMAL-VACUUM TEST

MIT Lincoln Laboratory informed Fairchild Republic that they developed and subsequently assembled at CSI, Mylar energy storage capacitors which could, upon a small modification of the capacitor-thruster test rig, be used in the new test rig that was fabricated.

MIT Lincoln Laboratory subsequently provided as GFE to Fairchild Republic three Mylar energy storage capacitors built to their stringent specification and quality assurance efforts. Fairchild Republic potted the anode bushing assembly and also provided the capacitor with a black thermal coating. The capacitor-thruster test rig shown in Figure 4 was modified in order to replace the CSI capacitors by the MIT provided capacitors. Since the MIT capacitors did not have threaded anode studs, a bushing adaptor had to be machined in order to accommodate the capacitor to the test rig.

Since a smaller vacuum chamber (4-ft. x 6-ft.) became available ahead of the scheduled larger (6-ft. x 8-ft.) vacuum chamber, it was decided to install the capacitor-thruster test assembly in the smaller chamber and perform the required testing within the pumping limitations of the smaller chamber. The test data revealed that this small chamber had sufficient pumping capability to operate the thruster at a maximum input power to the capacitor of 133 watts under radiation cooled conditions at roughly 16.4 joules/lb. and just reach the maximum preferred capacitor temperature (actually this latter temperature was exceeded by 1°F). As one might expect, under conduction cooled conditions (a sink temperature of 60° to 62°F, i.e., 15.6 to 16.7°C) it would have been possible to operate the thruster well above the 133-watt input power load if a larger vacuum pumping capability had been available. The test program carried out was successful since it was possible to obtain both radiation and conduction cooled thermal vacuum data at the same power level with one of the three power levels of operation being about 100 watts. The lower power level tested was roughly 75 watts and the upper roughly 130 watts. In all cases the capacitor energy density tested was about 16.4 joules/lb.

Table 6 presented the location of the seven thermocouples located on the test rig. Figures 6 through 8 present the temperature history as a function of time for the radiation cooled thermal vacuum test condition and three different power levels of operation. Figures 9 through 11 present the corresponding results for the conduction cooled condition.

Table 10 summarizes the test results.

An examination of the data presented in Figures 6 through 11 revealed that, due to the temperature gradient, thermal energy is conductively transferred from the anode electrode in the direction of the capacitor via the copper strip line assembly. Some thermal energy is lost via radiation along this strip. Even though thermal energy is lost, some reaches the ground ring and one notes the temperature at the capacitor ground ring to be higher than the temperature at the cylindrical side face (and back face) of the capacitor. Since no thermocouples were located inside the capacitor it cannot be established whether or not a temperature gradient also exists inside the capacitor. It is suspected however, that due to the construction of the capacitor, thermal energy is transferred more readily along the exterior metal

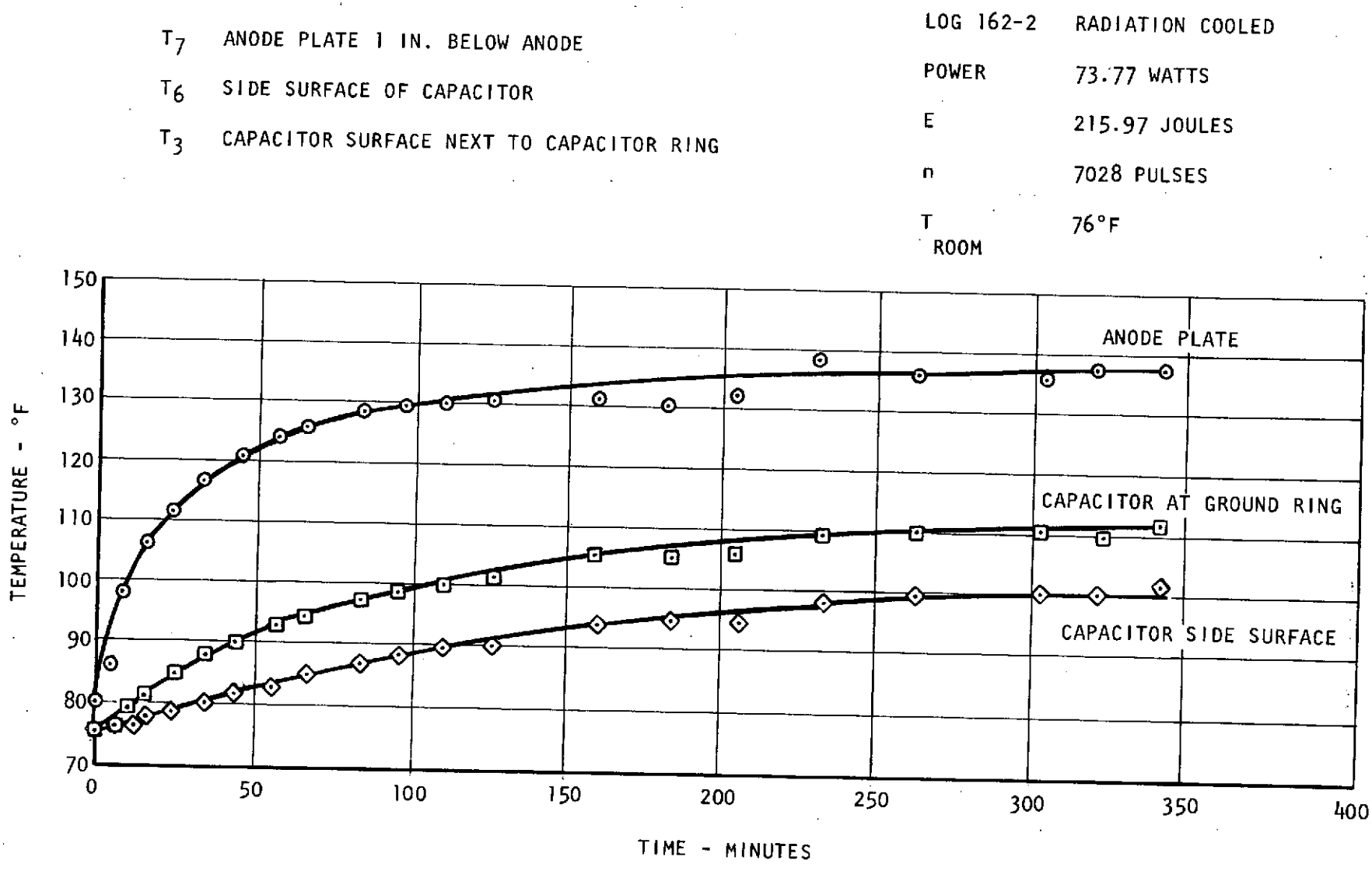

Figure 6. Radiation Cooled Thermal-Vacuum Temperature History (73.77 watts)

		LOG 166-3	RADIATION COOLED
T_7	ANODE PLATE	POWER	97.00 WATTS
T_6	SIDE SURFACE OF CAPACITOR	E	223.2 JOULES
T_3	CAPACITOR SURFACE NEXT TO CAPACITOR GROUND RING	n	9594 PULSES
		T_{ROOM}	76°F

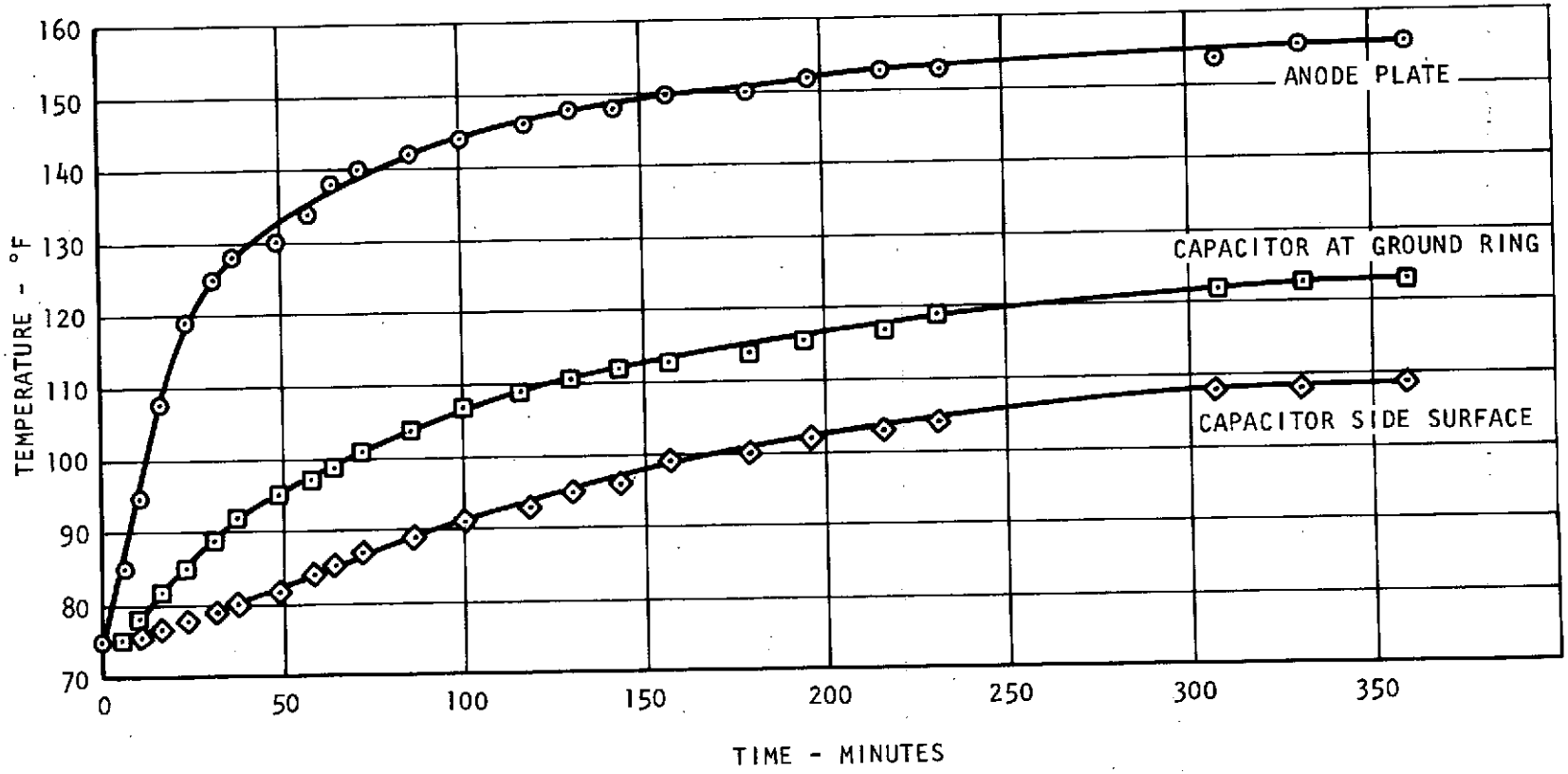

Figure 7. Radiation Cooled Thermal-Vacuum Temperature History (97.00 watts)

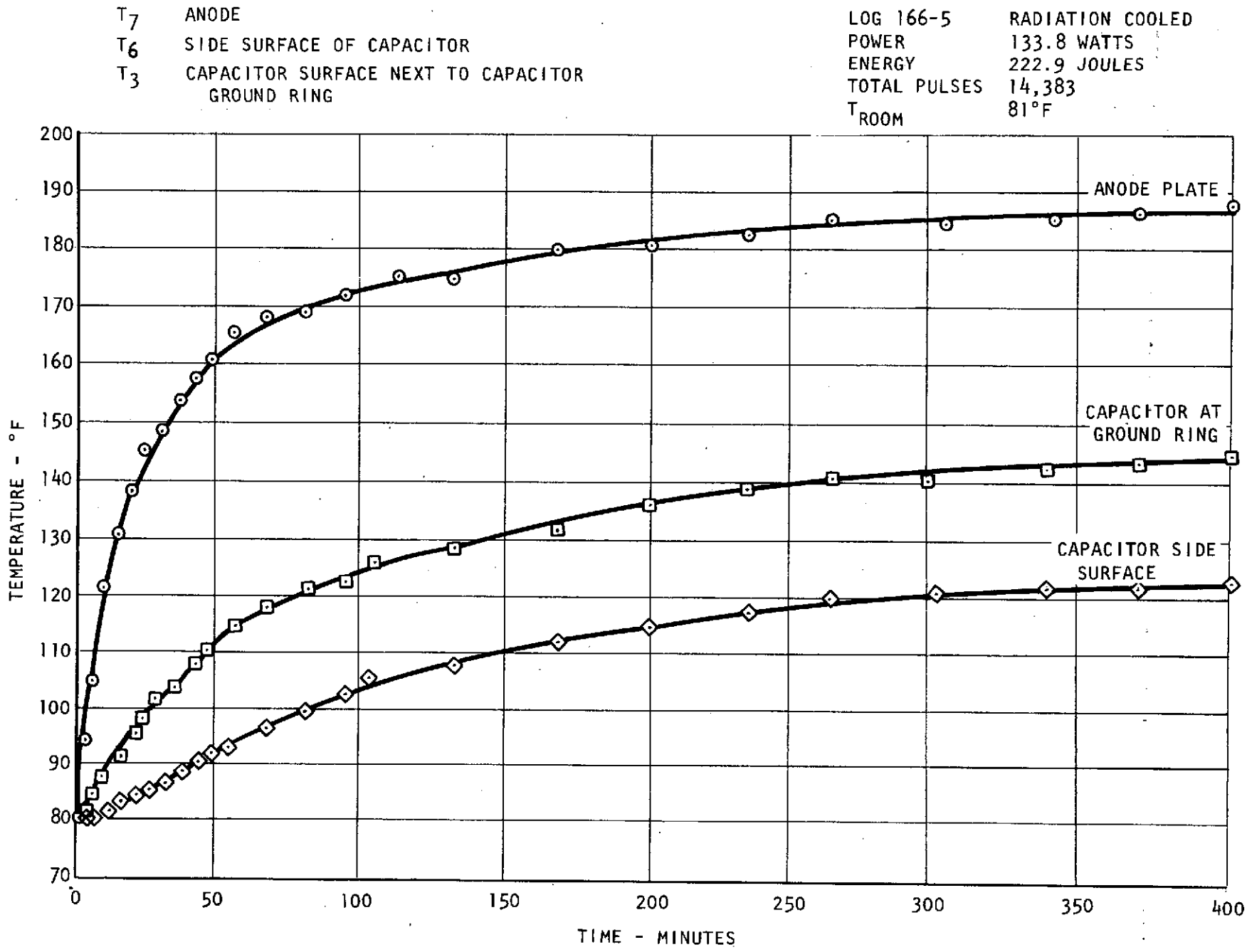

Figure 8. Radiation Cooled Thermal-Vacuum Temperature History (133.8 watts)

T_7 ANODE PLATE

T_6 SIDE SURFACE OF CAPACITOR

T_3 CAPACITOR SURFACE NEXT TO CAPACITOR GROUND RING

POWER 75.4 WATTS

ENERGY 222.9 JOULES

PULSES OF TEST 7224

T_{SINK} 60°F TO 61°F

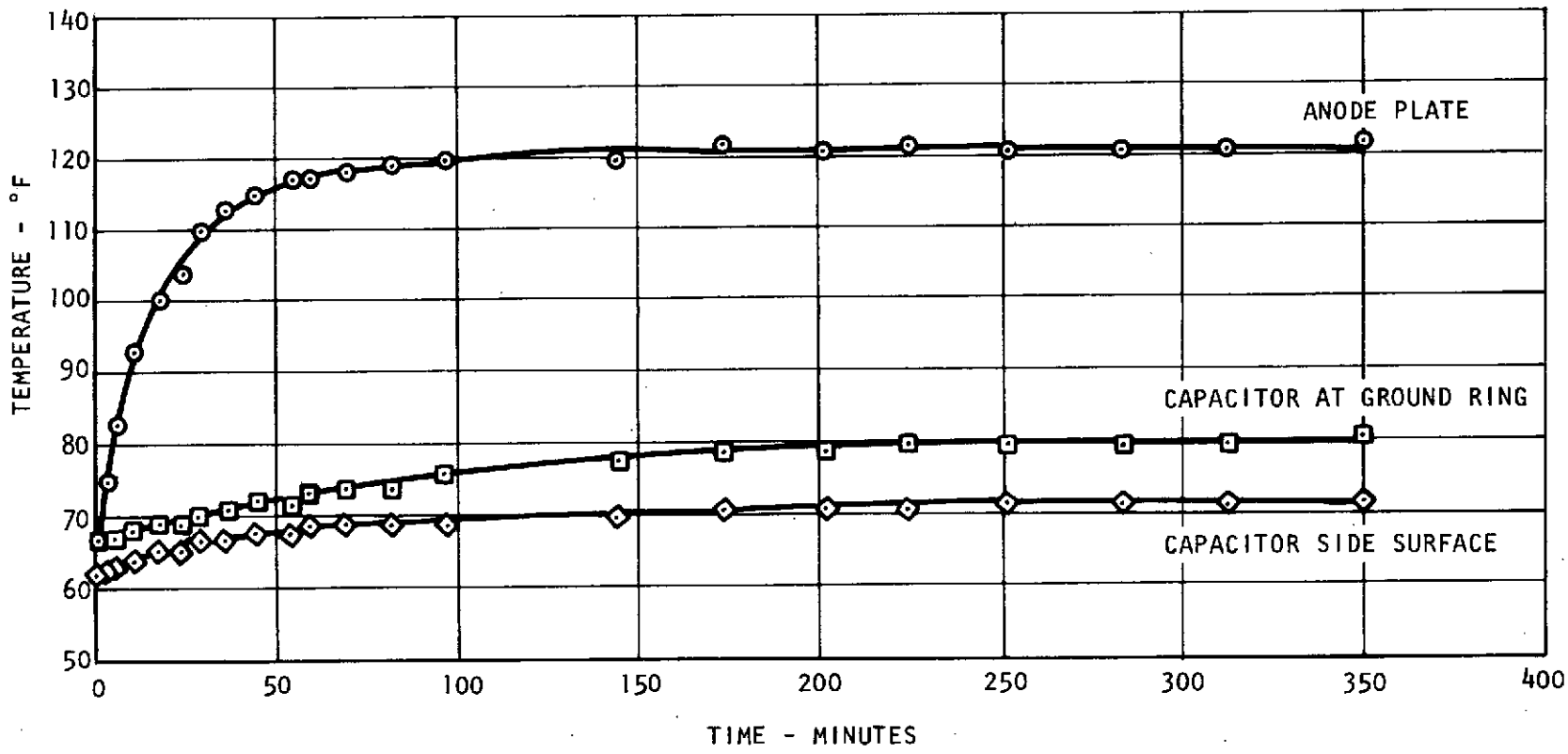

Figure 9. Conduction Cooled Thermal-Vacuum Temperature History (75.4 watts)

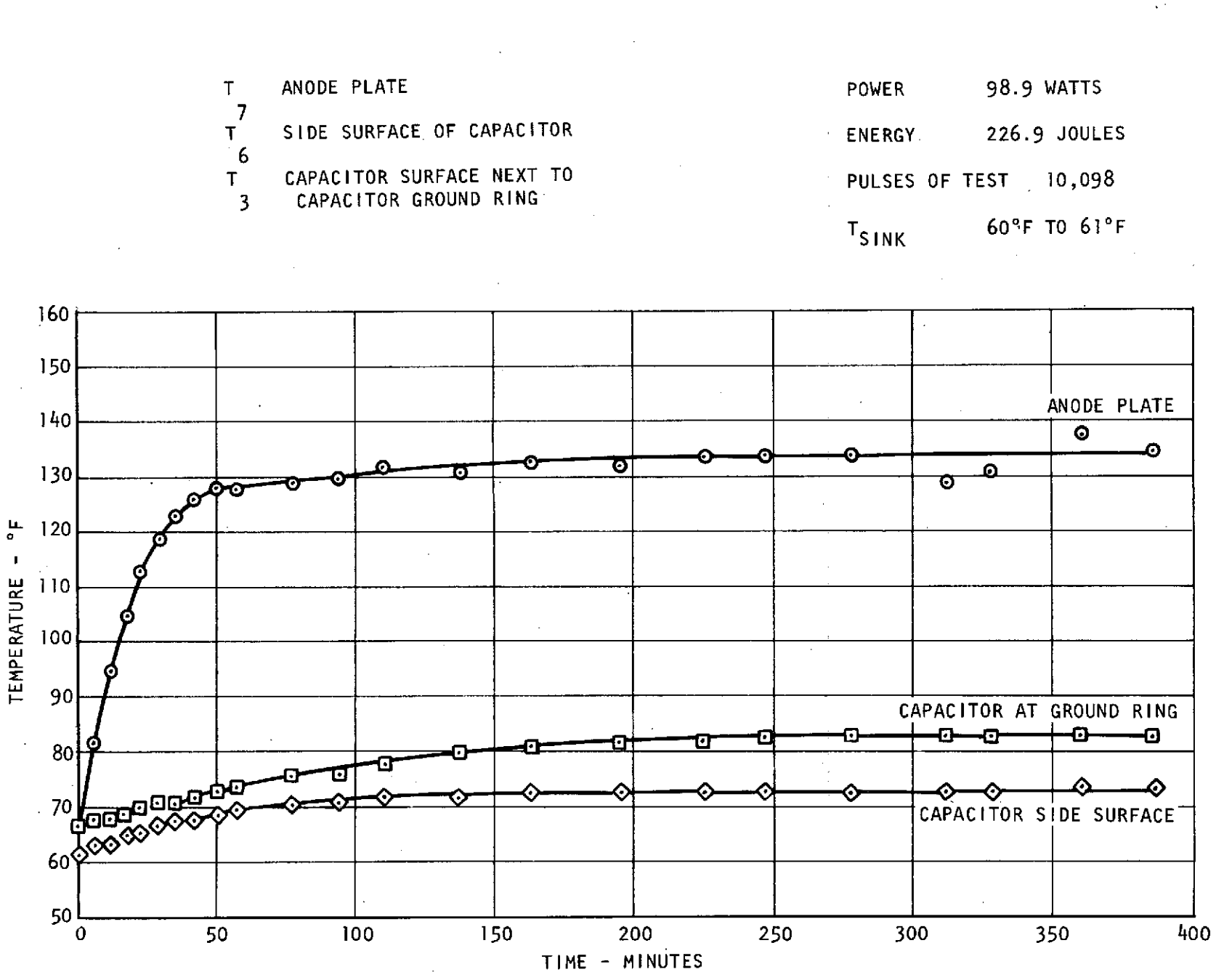

Figure 10. Conduction Cooled Thermal-Vacuum Temperature History (98.9 watts)

T_7 ANODE PLATE

T_6 SIDE SURFACE OF CAPACITOR

T_3 CAPACITOR SURFACE NEXT TO GROUND RING

T_1 CATHODE PLATE (WATER COOLED SINK)

POWER	129.2 WATTS
ENERGY	214.7 JOULES
TOTAL PULSES	14,771
T_{SINK}	60°F TO 62°F

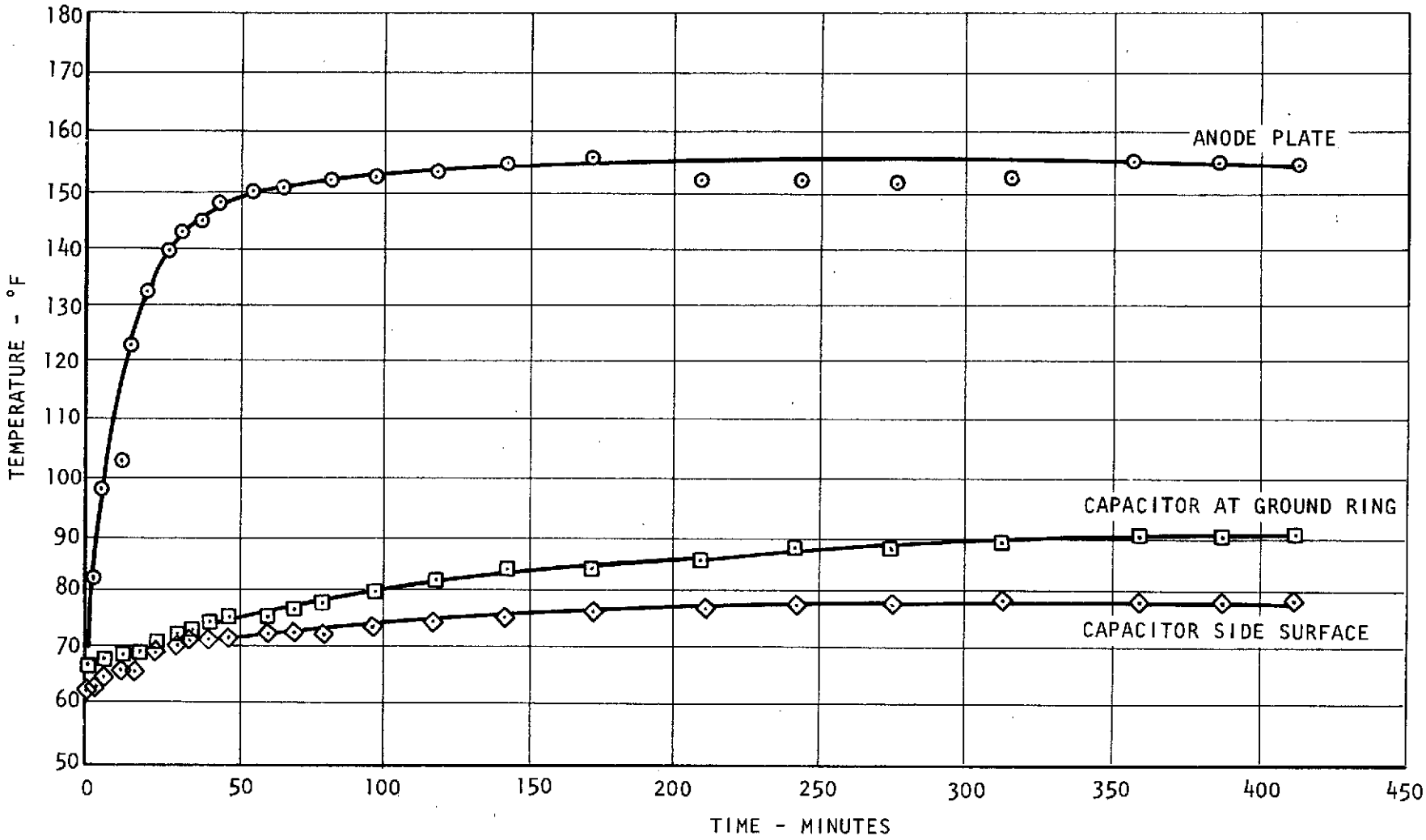

Figure 11. Conduction Cooled Thermal-Vacuum Temperature History (129.2 watts)

TABLE 10. SUMMARY OF TEST RESULTS
(EQUILIBRIUM TEMPERATURES)

Log	Power (w)	T_2 Anode Plate	T_3 Ground Ring	T_6 Capacitor Side	T (Sink Temp)
166-2	73.77 watts	(137°F)58.3°C	(111°F)43.9°C	(100°F)37.8°C	(76°F) room 24.4°C
166-3	97.00 watts	(156°F)68.9°C	(123°F)50.6°C	(109°F)42.8°C	(76°F) room 24.4°C
166-5	133.8 watts	(188°F)86.7°C	(145°F)62.8°C	(123°F)50.6°C	(81°F) room 27.2°C
166-6	129.2 watts	(158°F)70°C	(90°F)32.2°C	(79°F)26.1°C	(60-62°F) 15.6-16.7°C
166-7	98.9 watts	(134°F)56.7°C	(83°F)28.3°C	(73°F)22.8°C	(60-61°F) 15.6-16.7°C
166-8	75.4 watts	(121°F)49.4°C	(80°F)26.7°C	(72°F)22.2°C	(60-61°F) 15.6-16.7°C

case of the capacitor rather than into the capacitor through the ceramic bushing and the small anode stud. In any case it is clear that care must be exercised in the vacuum testing of pulsed plasma thrusters to preclude the possibility of the capacitor from becoming overheated due to heat transferred from the electrodes to the capacitor along the strip lines. The worse case tested corresponded to the highest power level of 133.8 watts under radiation cooled conditions. The data of this test is presented in Figure 8. The sink temperature of the vacuum chamber was essentially room temperature (81 °F = 27.2 °C). The capacitor equilibrium temperature of 50.6 °C (123 °F) could be tolerated without seriously affecting capacitor life. It must therefore be concluded that even under radiation cooled conditions the high energy solid propellant pulsed plasma thruster can be operated at input power levels which are compatible with the maximum electric power levels that presently could be allocated to an electrical propulsion system aboard a spacecraft. Indeed, from the equilibrium temperature data as a function of input power (Figure 12) one can see that if a suitable heat sink is provided, thruster operation well above 130 watts would be possible before the capacitor temperature would become a limiting factor in thruster operation.

Discharge voltage and current data were also taken during the thermal vacuum tests. Table 11 presents the results of the data.

TABLE 11. PEAK DISCHARGE CURRENT DATA

Log	Initial Voltage	Peak Discharge Current	Input Power
Radiation Cooled			
166-2	2899.4	72,285 amps	73.77 watts
166-3	2948.3	73,333 amps	97.00 watts
166-5	2945.8	74,577 amps	133.8 watts
Conduction Cooled			
166-6	2890.7	73,987 amps	129.2 watts
166-7	2971.7	72,550 amps	98.9 watts
166-8	2947.8	74,174 amps	75.4 watts

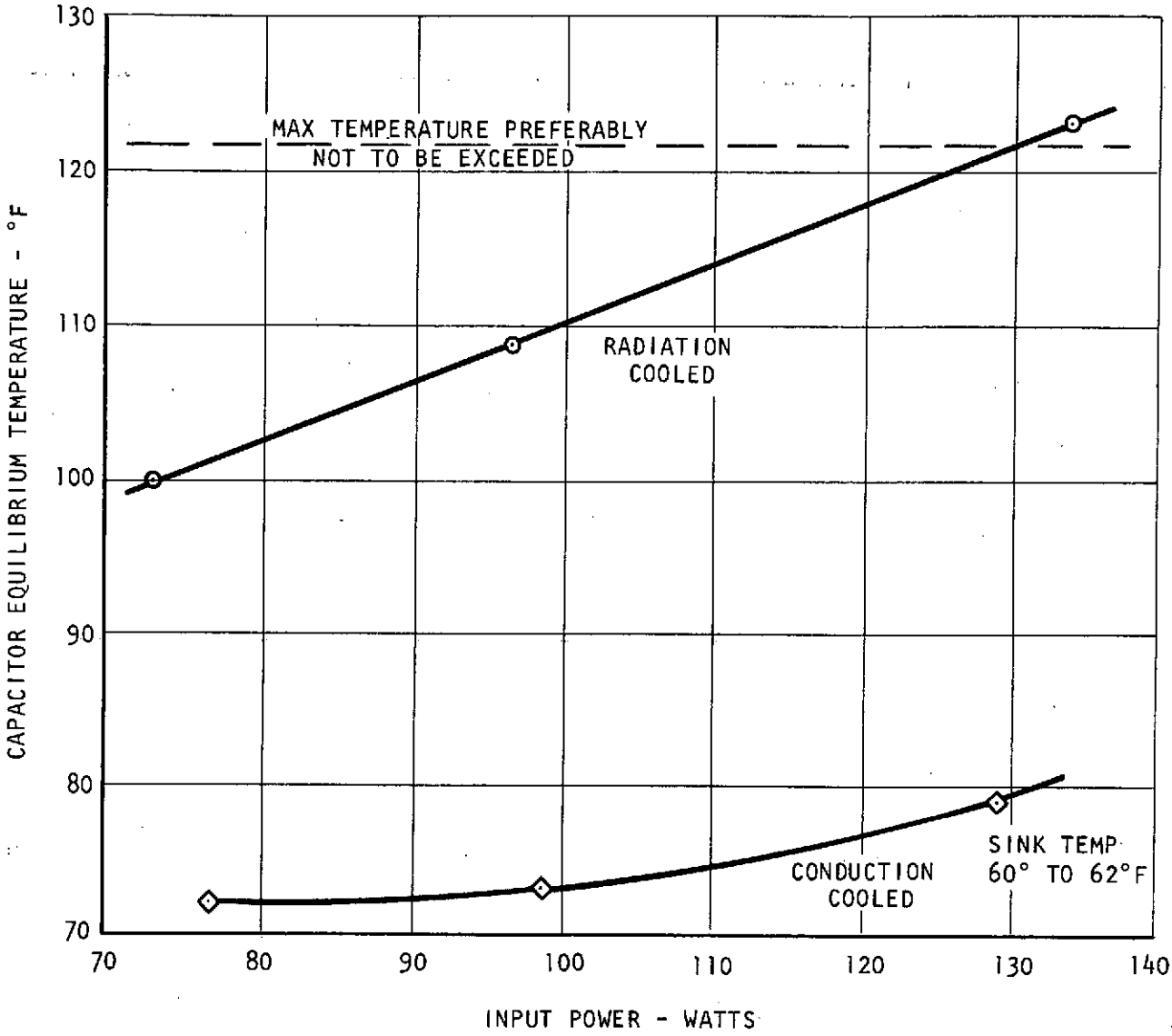

Figure 12. Equilibrium Temperature as a Function of Input Power

The voltage variations noted during the test were due to the use of a non-regulated power supply and the inability to hold voltage absolutely constant. Since the discharge energy was very nearly the same for all 6 tests, the peak discharge current is also seen to be essentially the same for all tests. Input power during testing was varied merely by varying the pulse frequency of thruster firing.

3.3 PROLONGED OPERATION IN A VACUUM

Program requirements called for initiating a life test under vacuum conditions of the high energy density capacitor using a typical pulsed plasma thruster nozzle as the load. The test duration was to have a minimum duration of at least four weeks.

The required vacuum life test was initiated upon completion of the thermal-vacuum tests described in Section 3.2. The life test was carried out under radiation cooled conditions at a pulse rate of about 0.5 Hz and an energy density of about 16.4 joules/lb. The power level of operation was roughly 110 watts.

Temperature, discharge current and discharge voltage were monitored during the test. While not required, solid propellant consumption was also monitored and recorded during the test.

Table 12 presents the temperature data recorded during the life test. The thermocouple locations are presented in Table 6. The capacitor temperature (T6) was about 5°F to 6°F (i.e., about 3°C) below the maximum "allowable" temperature of 122°F (50°C). Thus, it can be concluded that the power level of the test (about 110 watts) represented a completely safe power level of operation. Table 13 presents a listing of the pulse frequency checks that were carried out. The average pulse rate of the test was about 0.5117 Hz.

The peak discharge currents monitored during the test are presented in Table 14.

Table 15 presents a summary of the total number of discharges that were accumulated on the MIT Lincoln Laboratory provided high energy density capacitors.

As far as is known, the extended life test performed presently represents the longest test of a large total impulse bit pulsed plasma thruster reported and the results of the test are believed to represent a major advancement in the state-of-the-art of pulsed plasma thrusters.

TABLE 12. TEMPERATURE DATA DURING VACUUM LIFE TEST
(Radiation Cooled Test)

Date	Pulse Count	Total Fuel Used (inches)	T1 °C(°F)	T2 °C(°F)	T3 °C(°F)	T4 °C(°F)	T5 °C(°F)	T6 °C(°F)	T7 °C(°F)
1/3/74	0	0							
1/4/74	29,665	0.12	58.3(137)	56.1(133)	56.7(134)	56.7(134)	54.4(130)	47.2(117)	77.2(171)
1/7/74	157,298	0.64	57.2(135)	55 (131)	56.1(133)	56.1(133)	53.9(129)	56.1(115)	77.8(172)
1/8/74	200,408	0.81	58.3(135)	55.6(132)	56.1(133)	56.1(133)	54.4(130)	46.7(116)	78.3(173)
1/9/74	244,080	0.99	58.3(135)	55 (135)	56.1(133)	56.1(133)	53.9(129)	46.1(115)	77.8(172)
1/10/74	287,198	1.15	58.3(135)	55 (131)	56.1(133)	56.1(133)	53.9(129)	46.7(116)	77.8(172)
1/11/74	300,482	1.30	57.8(136)	55.6(132)	56.7(134)	56.7(134)	54.4(130)	46.7(116)	77.8(173)
1/14/74	460,779	1.82	58.3(135)	55 (131)	56.1(133)	56.1(133)	53.9(129)	46.7(116)	77.2(171)
1/15/74	504,800	1.96	57.8(136)	55.6(132)	56.7(134)	56.7(134)	54.4(130)	46.7(116)	78.9(174)
1/16/74	549,600	2.13	58.3(137)	56.1(133)	57.2(135)	57.2(135)	51.7(125)	47.2(117)	79.4(175)
1/17/74	594,510	2.30	58.3(137)	56.1(133)	57.2(135)	57.2(135)	51.7(125)	47.2(117)	79.4(175)
1/18/74	639,436	2.48	58.3(137)	56.1(133)	57.2(135)	57.2(135)	51.7(125)	47.2(117)	78.9(174)
1/21/74	774,740	3.00	58.3(137)	56.1(133)	57.2(135)	57.2(135)	51.7(125)	47.2(117)	78.9(174)
1/22/74	819,145	3.17	57.8(136)	56.1(133)	56.7(134)	57.2(135)	54.4(130)	46.7(116)	78.9(174)
1/23/74	864,261	3.33	58.3(137)	56.7(134)	57.2(135)	57.2(135)	55 (131)	47.2(117)	79.4(175)
1/24/74	908,825	3.67	56.7(134)	54.4(130)	55 (131)	55.6(132)	53.3(128)	46.1(115)	75 (167)
1/25/74	953,372	3.83	56.7(134)	54.4(130)	55.6(132)	55.6(132)	53.3(128)	46.1(115)	75.6(168)
1/28/74	1,087,630	4.35	56.1(133)	54.4(130)	55 (131)	55 (131)	53.3(128)	45.6(114)	75 (167)
1/29/74	1,132,795	4.52	56.7(134)	54.4(130)	55.6(132)	55.6(132)	53.3(128)	46.1(115)	75.6(168)
1/30/74	-	4.70	56.1(133)	53.9(129)	54.4(130)	55 (131)	52.8(127)	46.1(115)	74.4(166)
1/31/74	1,222,765	4.88	58.3(135)	55 (131)	56.1(133)	56.1(133)	53.9(129)	46.7(116)	76.1(169)

TABLE 12. TEMPERATURE DATA DURING VACUUM LIFE TEST (continued)
(Radiation Cooled Test)

Date	Pulse Count	Total Fuel Used (inches)	T1 °C(°F)	T2 °C(°F)	T3 °C(°F)	T4 °C(°F)	T5 °C(°F)	T6 °C(°F)	T7 °C(°F)
2/1/74	1,267,795	5.05	58.3(135)	55 (131)	55.6(132)	56.1(133)	53.3(128)	46.1(115)	76.1(169)
2/5/74	1,421,344	5.70	58.3(137)	56.7(134)	57.2(135)	57.2(135)	51.7(125)	47.8(118)	80 (176)
2/6/74	1,466,510	5.72	59.4(139)	57.2(135)	58.3(137)	58.3(137)	56.1(133)	48.3(119)	80.6(177)
2/7/74	1,506,630	6.00	57.8(136)	55.6(132)	56.7(134)	56.7(134)	54.4(130)	47.2(117)	78.3(173)
2/11/74	1,654,067	6.67	58.3(137)	56.1(133)	56.7(134)	57.2(135)	51.7(125)	47.2(117)	78.3(173)
2/13/74	1,690,647	6.82	57.2(135)	51.7(125)	56.1(133)	56.1(133)	53.9(129)	47.2(117)	78.3(173)
2/14/74	1,733,927	7.01	58.3(137)	56.1(133)	56.7(134)	56.7(134)	51.7(125)	47.2(117)	78.9(174)
2/15/74	1,777,418	7.20	57.8(136)	55.6(132)	56.1(133)	56.7(134)	54.4(130)	47.2(117)	78.3(173)
2/19/74	1,946,173	7.87	57.8(136)	55.6(134)	56.1(133)	56.7(134)	53.9(129)	46.7(116)	80 (176)
2/21/74	1,989,729	8.04	57.8(136)	55.6(132)	56.1(133)	56.7(134)	54.4(130)	46.7(116)	78.9(174)
2/22/74	2,033,396	8.21	57.8(136)	56.1(133)	56.7(134)	57.2(135)	54.4(130)	47.2(117)	79.4(175)
2/27/74	2,196,132	8.76	59.4(139)	57.2(135)	57.8(136)	57.8(136)	56.1(133)	48.3(119)	(179)
2/27/74	2,197,610	System off for refueling							
3/1/74	2,231,504	8.90 total	58.3(137)	56.7(134)	57.2(135)	57.2(135)	55.6(132)	48.3(119)	(178)
3/4/74	2,364,075	9.44 total	58.3(137)	56.7(134)	(136)	(136)	55.6(132)	48.3(119)	(179)

TABLE 13. PULSE FREQUENCY CHECKS

Pulse Count	Pulse Frequency (Hz)
167	0.4995
209.433	0.5015
819,498	0.5176
909,556	0.5176
1,224,598	0.5222
1,692,844	0.5002
1,736,575	0.5056

TABLE 14. PEAK DISCHARGE CURRENT AMPLITUDE CHECKS

Pulse Count	Peak Discharge Current (amps)
595,367	72,285
876,261	67,571
910,178	69,928
1,237,829	68,749
1,693,035	73,856

TABLE 15. TOTAL SHOTS ON EACH OF THREE MITL/L PROVIDED HIGH ENERGY DENSITY CAPACITORS

Sum accumulated during all thermal tests	76,938
Sum of the pulses accumulated during the life test in progress	2,656,588
Total sum without failure	2,733,526

3.4 CONCLUSIONS AND RECOMMENDATIONS

It is now believed by Fairchild Republic that the poor vacuum life behavior of the CSI high energy density capacitors is not due to any of the various reasons claimed by the vendor. While the failure mechanisms put forth by the vendor are certainly normally valid failure mechanisms, the overwhelming evidence leads one to conclude that essentially all of the vacuum failures can be explained by the formation of a low pressure pocket inside the capacitor with a subsequent internal electrical breakdown resulting in failure. Early multi-pad capacitors received for testing were of an all welded construction. The welded seams most likely had microscopic pin holes in them. Later non-welded cylindrically shaped single pad capacitors had soft soldered seams with possible minute leakage paths from the interior of the capacitor to the exterior vacuum environment. The MIT Lincoln Laboratory provided capacitors featured a Helium leak tested vacuum brazed bushing assembly. Fairchild Republic provided a redundant epoxy seal on all of the seams of these capacitors thereby virtually precluding the presence of leakage paths. Capacitors with this latter type of composite construction did not exhibit an early type of failure such as had been encountered.

It is recommended that liquid impregnated energy storage capacitors for pulsed plasma thrusters intended for prolonged vacuum operation incorporate the following fabrication features:

1) The material of the capacitor can and back lid should be processed from hi-purity vacuum melt material with the grain size and inclusion content specified.

2) The bond (vacuum braze, etc.) between the high voltage bushing assembly and the capacitor can must be Helium leak tested to assure a leak tight assembly.

3) If feasible, the assembled capacitor should be Helium leak tested prior to the liquid impregnation process. Care should be exercised not to ingest contaminants into the capacitor during such tests.

4) All seams or joints, even if Helium leak tested, should preferably feature a redundant seal (i.e., an epoxy potting or capping technique).

4. ELECTROSTATIC AUGMENTATION STUDIES

4.1 BACKGROUND

Most of Fairchild Republic's studies of solid Teflon propellant pulsed plasma thrusters have been carried out with rail type and coaxial type electrode nozzles. Exploratory tests performed at Republic under Contract NAS1-10944 and also at MIT[6] have shown that the solid propellant thruster concept can also be extended to include conical electrode nozzle configurations. Such an electrode geometry has been extensively studied in Russia[7, 8, 9, 10, 11, 12]. A conical nozzle geometry has two features which potentially could improve pulsed plasma thruster performance:

1) The applied electrostatic field is oriented in the thrust producing direction.

2) Due to the large surface to volume ratio of such a geometry the amount of mass injected per discharge can be significantly increased when compared to either breech fed or V-shaped propellant side fed configurations.

The effect of the applied electrostatic field on plasma thruster performance was apparently first noted and reported by Burkhart at NASA Lewis while studying low power steady state MPD thrusters using gaseous propellants[13,14]. His primary observation was that upon placing the thruster cathode downstream of the anode one tends to eliminate an impressed electrostatic field which tends to accelerate ions toward the upstream backplate causing an ion loss. Furthermore, with a downstream cathode the impressed electrostatic field tends to accelerate ions out of the exhaust. Performance data presented in Reference 13 showed that an improvement in thruster performance could indeed be realized by this effect. Burkhart also takes advantage of a conically shaped magnetic field provided by coils and pole pieces.

Even though Burkhart obtained his results with a steady state gaseous propellant plasma thruster, the effects he observed are believed to hold for the solid propellant pulsed plasma thruster as well.

Three distinct sets of experiments were carried out at Republic to examine the effect of the electrostatic field on propulsion performance:

1) Effect of the Direction of the Electric Field (Electrode Polarity)

   This experiment examined the effect of the direction of the applied electric field on charged particles of the plasma during a discharge. The effect that Burkhart (Reference 13) observed for a steady state thruster was to be reexamined as it applied to a pulsed device. In one case the cathode was located downstream, in the second case upstream. Thruster performance data was compared for these two polarities.

2) Effect of the Amplitude of the Self-Applied Field

   Maintaining a constant energy of 350 joules, the number of capacitors and the initial voltage on them were varied while maintaining a fixed interelectrode spacing. Thruster performance data was compared.

3) Effect of an Auxiliary Electric Field

   An attempt was made to establish if a switched electric field supplied from a separate circuit could be used to transfer energy into the plasma during the plasma acceleration process.

The design of the conically shaped thruster nozzle was performed on the basis that efficiencies above 20% require a capacitor energy to propellant surface area ratio of about 100 joules/in^2. For a 300 joule discharge the required propellant area would therefore be about 3 in^2. Several Russian studies have been published on ablative accelerators using a conical propellant geometry. While a considerable body of information was presented in these papers, no information was presented on the relative trade-off between specific impulse and specific thrust as a function of the included cone angle. For lack of such data, a compromise was made in the present studies and the included cone angle was selected to be 40°. Some of the relevant details of the conical nozzle design are presented in Figure 13. Figures 14 and 15, respectively, present front and rear views of the thruster assembly mounted on a thrust balance.

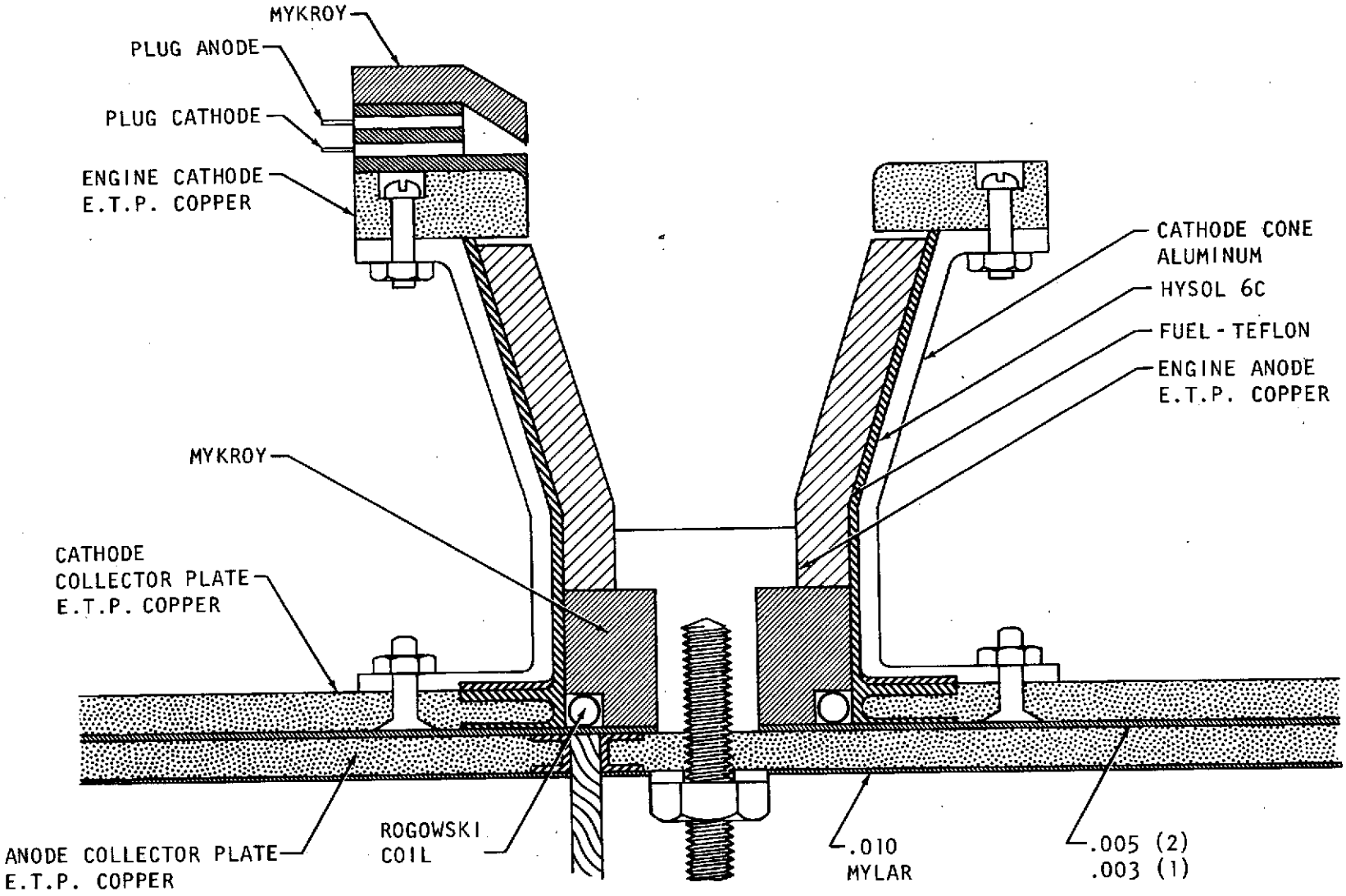

Figure 13. Details of Conical Nozzle Design

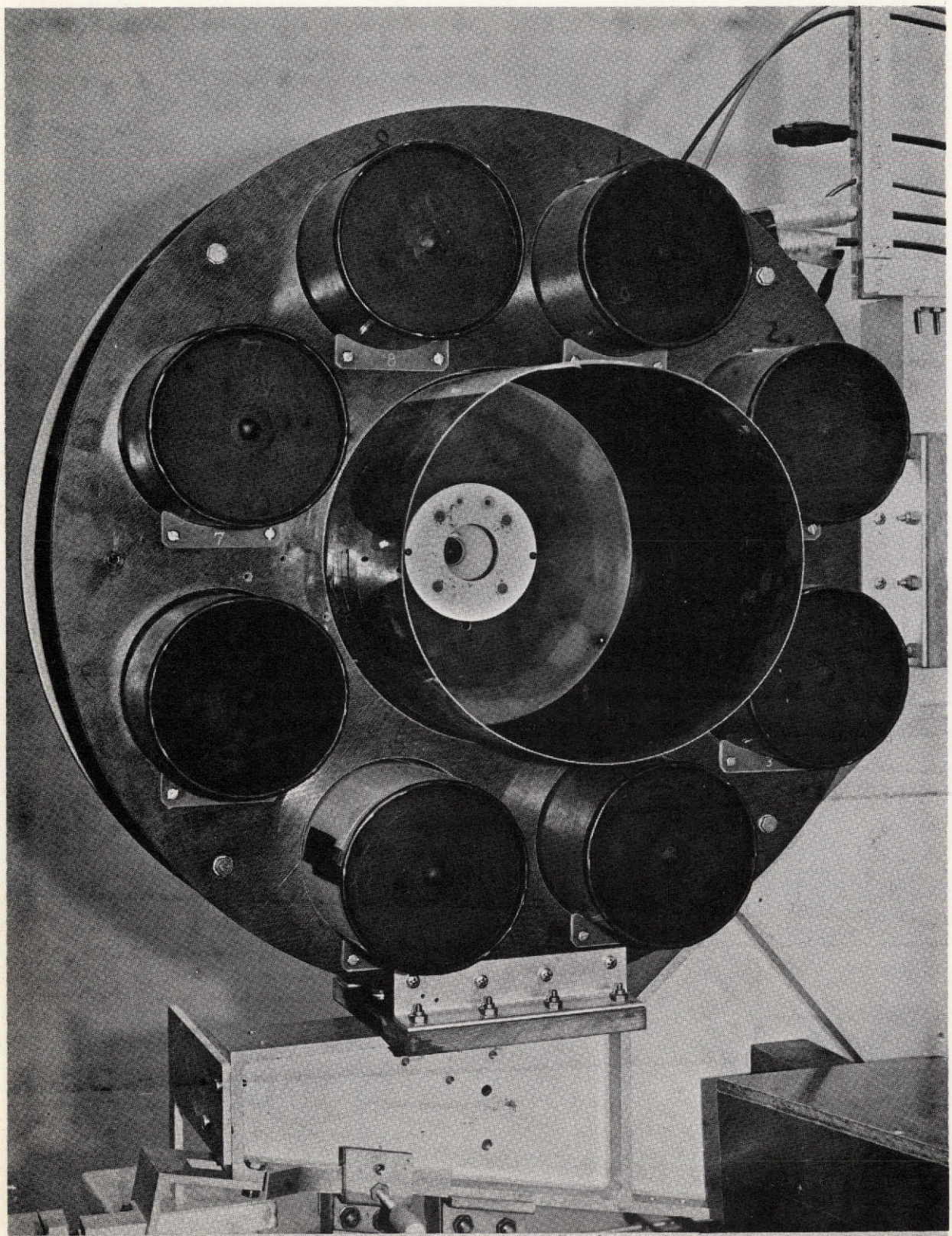

Figure 14. Front View of Conical Nozzle Thruster

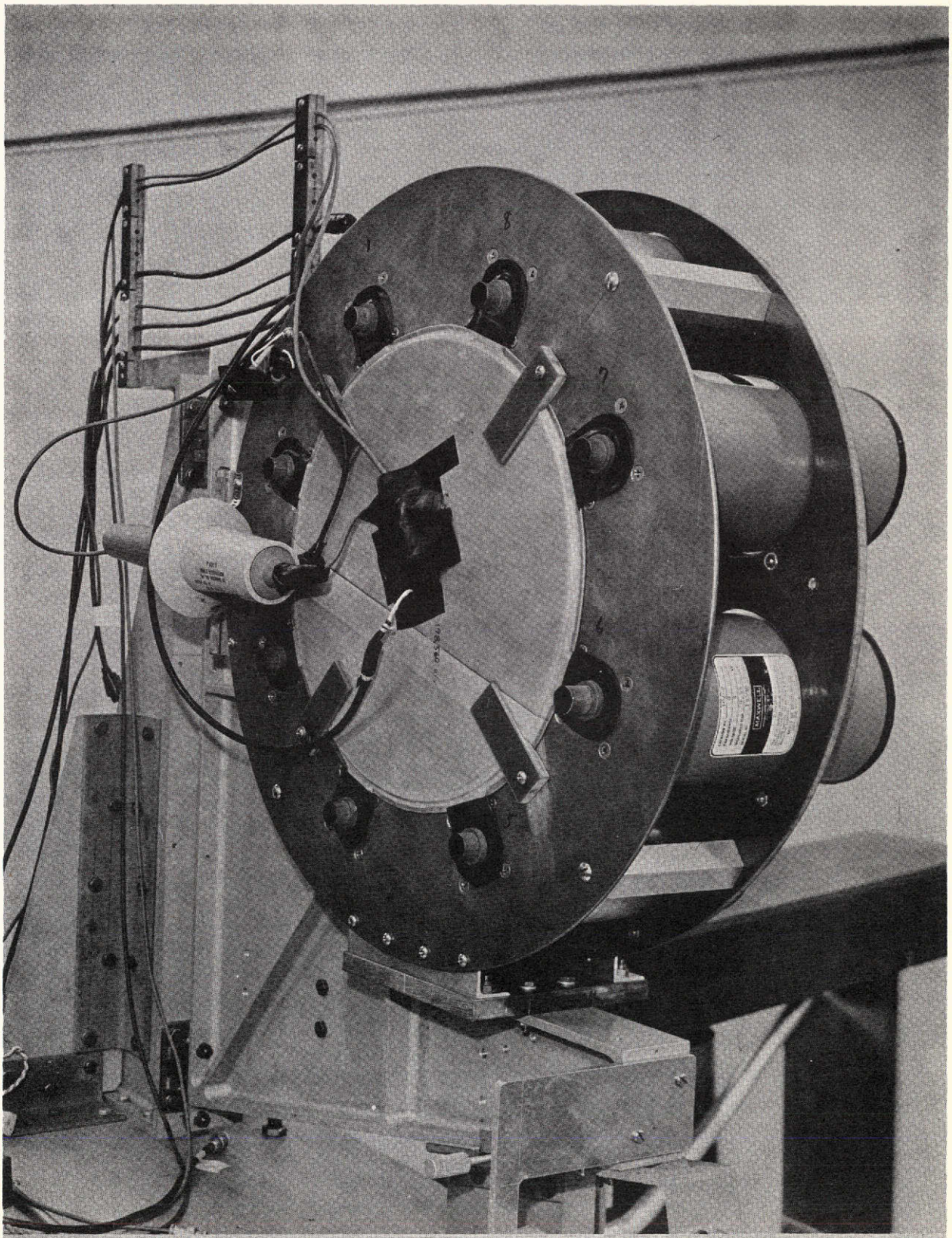

Figure 15. Rear View of Conical Nozzle Thruster

The thruster with the conically shaped nozzle was fabricated and a functional test was performed. The system met all expectations in that no localized arcing occurred under vacuum conditions and that an axially symmetric thruster discharge could be realized even though thruster ignition was initiated from one side of the nozzle. The first diagnostic test examining the effect of electrode polarity was subsequently carried out. This test involved the use of a downstream located cathode. Results of this test are presented in Table 16.

TABLE 16. EXPERIMENTAL RESULTS (LOG151-1)
CONICAL THRUSTER - CATHODE DOWNSTREAM

Initial voltage:	3.07 KV
Initial energy:	356 joules
Impulse bit amplitude:	2.848×10^{-3} lb-sec (12.668 milli-Newton-sec)
Impulse/Energy ratio:	8.00 milli-lb/KW (35.585 milli-Newton/KW)
Power /Thrust ratio:	125 watts/milli-lb
Specific impulse:	618.7 sec
Efficiency	10.79%

The measured performance differed from the calculated performance. Based upon the experience of breech fed and side fed propellant geometries, a thrust/power ratio of 6 milli-lb/KW (26.69 milli-Newton/KW) (167 watts/mlb = 37.54 watts/milli-Newton) at a specific impulse of about 1530 sec was expected. The expected thruster efficiency was 20%. Experimentally it was found that the conical configuration gave a higher thrust-to-power ratio than expected but at a much lower specific impulse than hoped for. It appears that similar to breech fed and side fed configurations, a limited number of experimental parametric studies would have to be performed with conical nozzle configurations before it becomes possible to design thrusters meeting a specific performance capability. Such parametric studies were beyond the scope of the program and therefore the studies were subsequently carried out with this given nozzle configuration.

4.2 EFFECT OF THE DIRECTION OF THE ELECTRIC FIELD (ELECTRODE POLARITY)

The direction of the electrostatic field in the conical electrode nozzle configuration is governed by the respective locations of the anode and cathode electrodes (see Figure 16).

The first experiment was performed with the electrode which is located at the apex of the cone being the anode and being at an initial voltage at +3070 volts (see Figure 16). The igniter plug was positioned in the ring-shaped cathode (i.e., negative ground) which was located at the exit plane of the conically shaped thruster barrel. The measured performance is presented in Table 17.

The electrode polarity was then reversed by using the downstream ring-shaped electrode as a positive ground with the negatively applied high voltage applied to the electrode at the apex of the cone (see Figure 16). In the latter field configuration it was found that the thruster capacitor could not be made to discharge. The direction of the electric field in this latter case inhibits thruster discharge initiation by means of surface igniter plugs. Evidently the microplasma produced by the igniter plugs is repelled by the applied electrostatic field and thus cannot "close" the discharge circuit. These two tests revealed that the direction of the applied electric field has a very marked effect on the ability to initiate a thruster discharge if the discharge is initiated by means of a microplasma producing igniter plug. It is interesting to note that this latter effect would not have been observed if a puff of neutral gas had been used to initiate the electric discharge.

The results of these two tests examining the effect of the direction of the electric field on performance are summarized in Table 17.

TABLE 17. POLARITY EFFECT ON PERFORMANCE

Test	Cathode	Anode	Specific Impulse	Efficiency
1	Downstream	Upstream	618.7 sec	10.79%
2	Upstream	Downstream	Thruster would not operate	

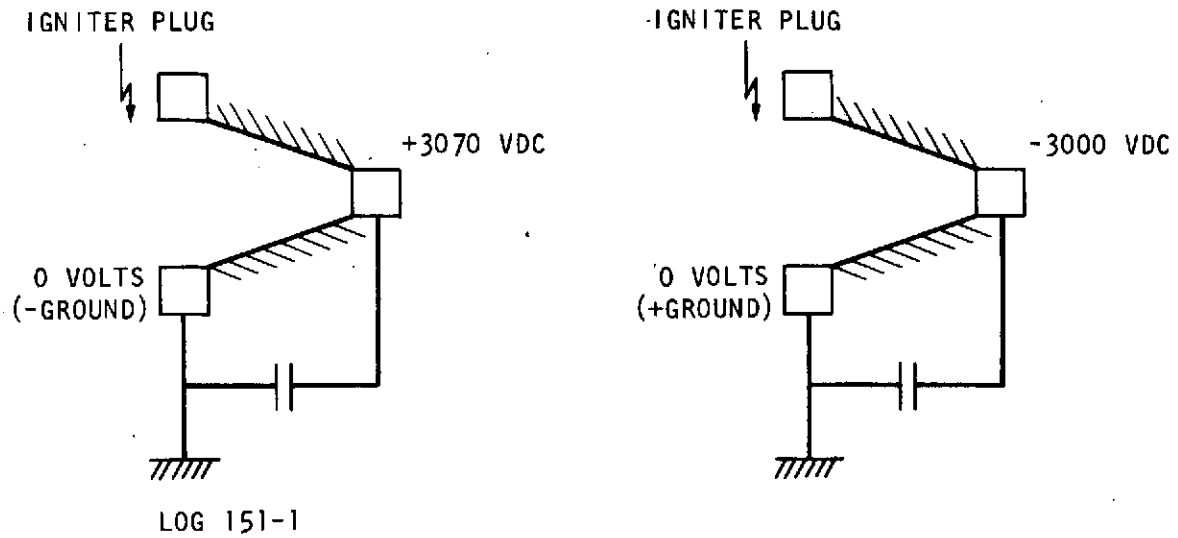

Figure 16. Location of Electrodes During Field Direction Tests

Another test which subsequently suggested itself, was to repeat the second test but relocate the igniter plug so that it is located in the upstream cathode. The electrode assembly was modified by opening a hole in the conically shaped return strap of the downstream electrode and also in the conically shaped Teflon propellant (see Figures 17 and 18). The hole in the return strap was located as close as possible to the upstream cathode and the material around the hole was electrically insulated so that the plasma could not return to the capacitor directly via the hole in the return strap. The igniter plug was potted so that only the discharge area of the igniter plug viewed the accelerator cavity of the conical thruster through the opening provided in the propellant and the back strap. After the igniter plug was moved into the vicinity of the cathode the question arose how to electrically interface the secondary of the thruster ignition electronic circuitry to the thruster discharge circuit. Normally, the cathode of an insulated igniter plug is electrically connected to the thruster cathode through a 1 ohm resister. Since the cathode of a normal polarity configuration is at ground potential, no electrical insulation problems arise. However, in the new reversed polarity configuration that was to be evaluated, the cathode will be at a negative potential relative to the positive ground and the negatively applied voltage will appear statically on the secondary windings of the pulse transformer of the discharge initiating circuit. It was learned from the vendor of the transformer that besides the +500 volt pulse applied to the primary of the transformer, an initial -2 KV static voltage could be safely applied to the secondary winding. Because of the posible danger involved in using the available pulse transformer in this latter manner, an exploratory test was performed with the secondary of the transformer connected to the positive ground. As expected, the thruster discharge could not be initiated even though the igniter plug fired. Furthermore, a discharge could not be initiated by floating the secondary of the pulse transformer circuit. These latter observations reconfirmed the previous test results that electrostatic field effects do affect the thruster discharge initiation process. With the transformer secondary connected to the cathode (negative potential) a thruster discharge could be initiated reliably and repeatedly with the reversed polarity. Since the earlier normal polarity tests of the conical configuration were performed at about 3 KV, Table 16, it was realized that because of the -2 KV limitation on the pulse transformer it would not be possible to obtain performance data of the reverse polarity configuration at the same energy level as the earlier studies. In order to obtain a meaningful comparison between the two polarities,

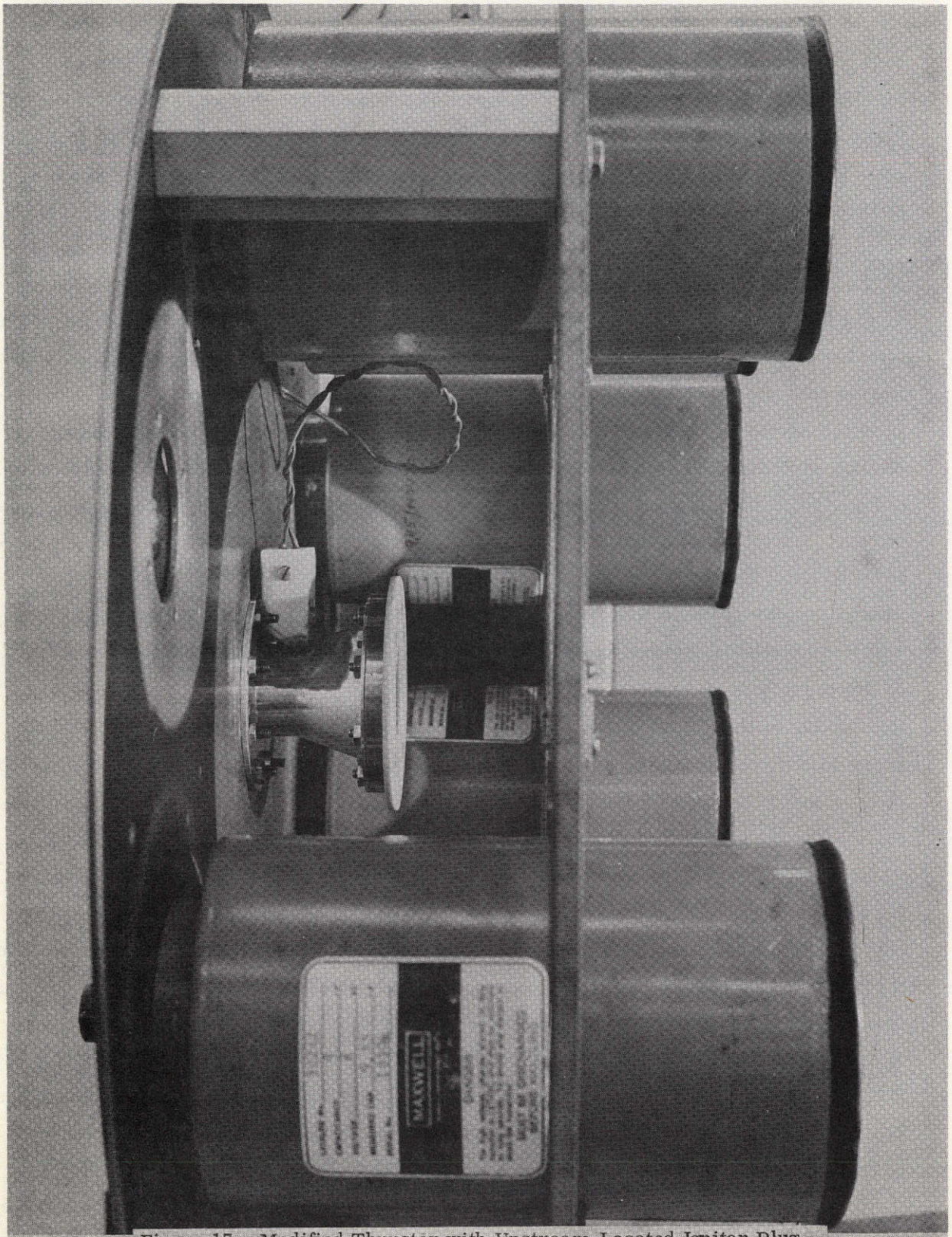

Figure 17. Modified Thruster with Upstream Located Igniter Plug

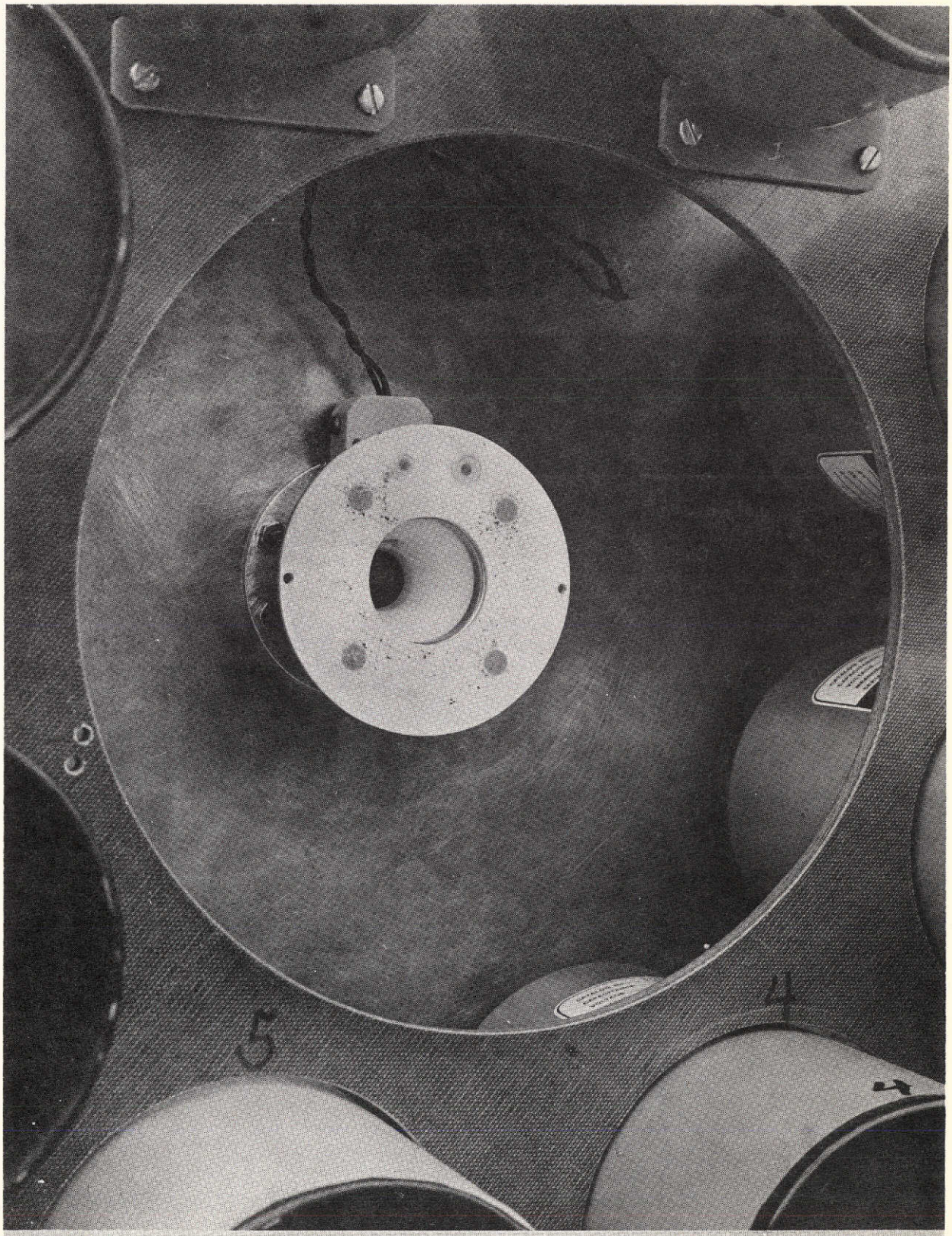

Figure 18. Conical Nozzle with Upstream Located Igniter Plug

both polarities would have to be examined at the lower energy level. Two tests (Log 151-11 and 151-12) were therefore performed at a lower energy level. Table 18 presents the results of these tests.

TABLE 18. POLARITY TEST RESULTS

Log	151-11	151-12
Upstream polarity	Negative	Positive
Upstream potential	-2196 V	+2228 V
Downstream potential	+ground (0 V)	-ground (0 V)
Discharge energy	183.1 j	188.5 j
Impulse bit amplitude	1.268×10^{-3} lb-sec	1.257×10^{-3} lb-sec
Impulse/energy ratio	6.925 mlb/Kw	6.67 mlb/Kw
Power/thrust ratio	144.4 w/mlb	149.9 w/mlb
Specific impulse	514 sec	515.6 sec
Thrust efficiency	7.76%	7.49%

Table 19 is presented in order to be able to make a better comparison of the test results that were obtained.

TABLE 19. COMPARISON OF TEST RESULTS

Energy Ratio E_a/E_b	0.971
Impulse Bit Ratio I_a/I_b	1.009
Impulse/Energy Ratio $(I/E)_a/(I/E)_b$	1.038
Specific Impulse Ratio Isp_a/Isp_b	0.997
Efficiency Ratio η_a/η_b	1.036

Subscripts a and b in Table 19 denote the data of Log 151-11 and Log 151-12, respectively. The results presented in Table 19 suggest that no real difference exists between the two sets of data. This result was found to be rather surprising in

view of the results of the extensive work of Burkhardt using a steady-state low power plasma accelerator. An interpretation of the results that were obtained will be presented in Section 4.5 of this report.

4.3 EFFECT OF THE AMPLITUDE OF THE SELF-APPLIED FIELD

The performance as effected by the amplitude of the initial longitudinal electric field was examined at a constant discharge energy of about 350 joules. The amplitude of the initial electric field was varied at constant energy by changing voltage and capacitance. The interelectrode spacing was kept constant and the cathode was located downstream. The results of these tests are presented in Table 20.

TABLE 20. ELECTRIC FIELD STRENGTH TESTS

Log	151-1	151-7	151-4	151-6	151-6
Number of capacitors	8	8	6	6	4
Initial voltage	3070	3046	3556	3540	4271
Volts/cm	1059	1050	1226	1221	1473
Initial energy, J	356	350.7	358	355	343.4
Impulse bit, lb-sec	2.848×10^{-3}	2.887×10^{-3}	2.944×10^{-3}	2.814×10^{-3}	3.012×10^{-3}
Thrust/ power, mlb/kW	8.00	8.23	8.22	7.92	8.77
Power/ thrust, W/mlb	125.0	121.5	121.6	126.2	114.0
Specific impulse, sec	618.7	618.7	635	580	605
Efficiency	10.79	10.55	11.38	10.0	11.57
$E/\bar{E}$	1.0009	0.994	1.015	1.007	0.974

The conclusion reached is that if performance is effected by the amplitude of the initially applied electrostatic field, it could not be detected in the range whose field strength varied from 1050 volts/cm up to 1473 volts/cm and at the low specific impulse values of the tests. Geometric parameters generally have been found to have a more pronounced effect on performance than those effects observed. The only two correlations that apparently were found to apply reasonably well are:

a) The correlation between the energy/impedance ratio and $\int i^2 dt$

b) The correlation between the mass per discharge and $Ap/Ao \int i^2 dt$

These correlations are shown in Table 21.

TABLE 21. CORRELATIONS OBSERVED

Log	$\int i^2 dt$	Eo/Zo	$Ap/Ao \int i^2 dt$	m
151-4	70,839	20.9×10^{-3}	172.2×10^{3}	4.628×10^{-6}
151-6	74,390	21.5×10^{-3}	180.8×10^{3}	4.849×10^{-6}
151-1	76,259	25.4×10^{-3}	185.4×10^{3}	4.598×10^{-6}
151-5	79,714	16.2×10^{-3}	193.8×10^{3}	4.969×10^{-6}
151-7	81,880	25.8×10^{-3}	199.1×10^{3}	4.911×10^{-6}

4.4 EFFECT OF AN AUXILIARY ELECTRIC FIELD

Extensive tests with an externally applied electrostatic field were performed in order to evaluate the effect of such a field on performance. A block diagram of the technique that was implemented is presented as Figure 19. Basically, two independent power supplies are used. One power supply (PS1) is used to charge up the capacitor bank of the thruster. The initial electrostatic field due to the charged capacitor bank is, therefore, applied across the conically shaped electrode, with the downstream ring-shaped electrode being the cathode which is at ground potential. A second power supply (PS2) having a positive ground is used to apply a large negative electrostatic field in the region of the ground electrode (i.e., cathode) of the

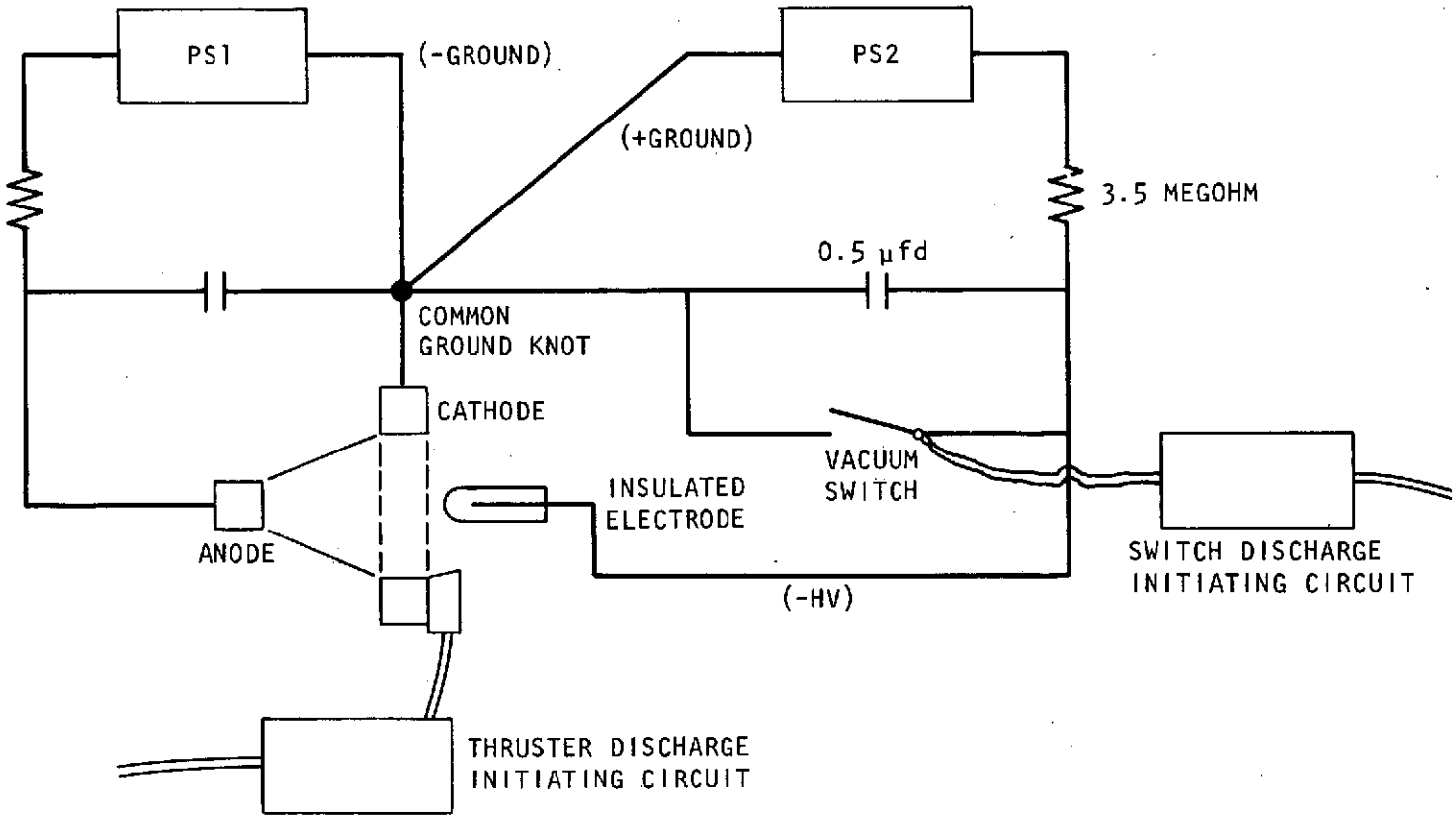

Figure 19. Block Diagram of Equipment Used for Externally Applied Electrostatic Field Experiments

thruster. This latter field is applied by connecting the negative high voltage output of this second power supply to an electrically insulated electrode mounted in the vicinity of the ground electrode (cathode) of the thruster. Whereas the applied potential of the main capacitor bank drops rapidly as the arc is generated, the potential of the externally applied field can be maintained at a relatively large value independent of that of the main thruster.

In order to be able to rapidly remove the externally applied electrostatic field it was necessary to develop a vacuum switch which could, upon command, rapidly remove the externally applied potential. This latter requirement was believed necessary since the accelerated plasma would initially be moving in one direction relative to the externally applied field and subsequently in the opposite direction to it as it passes the shielded electrode. A sketch of the vacuum switch that was developed is shown as Figure 20.

In order to determine if energy is transferred to the plasma by means of the externally applied electrostatic field, the output of the second power supply (PS2) was connected across a small (0.5 μfd) high voltage capacitor. This capacitor was connected directly across the downstream ground electrode of the thruster and the insulated external field electrode. A Tektronix high voltage probe was used to record the instantaneous voltage on the capacitor. It was reasoned that if energy is transferred into the plasma via the electrostatic field, the energy would have to be supplied by this capacitor. A 3.5 Megohm resistor was used between the power supply (PS2) and the capacitor to preclude the possibility of the power supply supplying any measurable amount of energy to the capacitor during a thruster discharge.

A number of subsystem tests were performed before the subsystems were integrated to the thruster in accordance with Figure 20. The first series of tests were concerned with demonstrating that the vacuum switch and the external field circuit could be operated independent of the main thruster discharge circuit. These tests were performed in a vacuum bell jar. Upon command, it was possible to discharge the 0.5 μfd capacitor rapidly to zero volts using a positive ground on the power supply (PS2) for the 0.5 μfd capacitor and a negative ground on the power supply required for the discharge initiating circuit of the switch igniter plug.

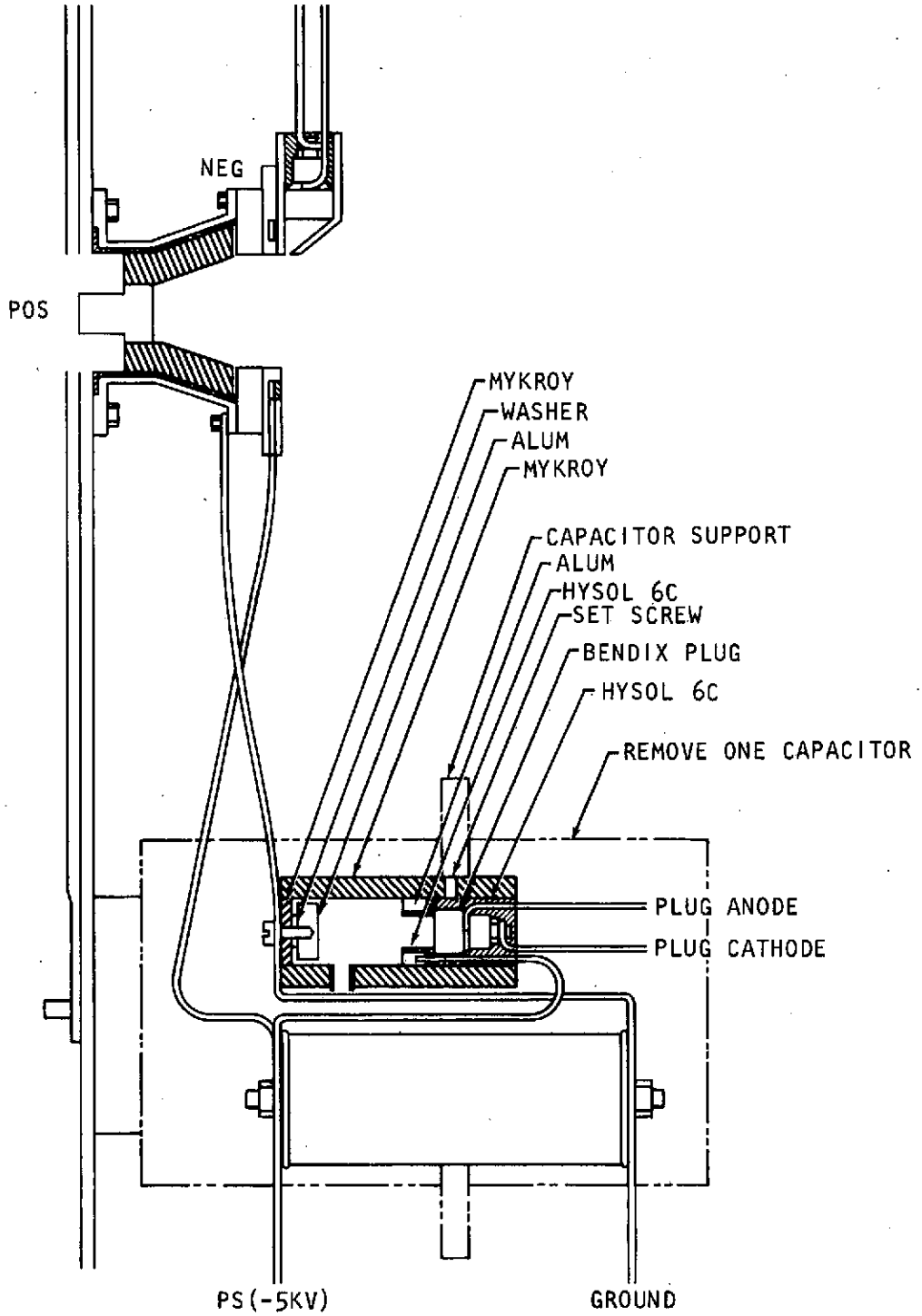

Figure 20. Sketch of Vacuum Switch Integrated to Thruster

After integrating the external field circuit to the conical thruster that was used for the earlier electrostatic field studies of the program, the following tests were performed:

1) Operation of only the main thruster

2) Operation of only the external field circuit

3) Both systems operated together

These tests verified that no ground loops or other problems were introduced by connecting the negative ground of the thruster power supply (PS1) to the positive ground of the external field power supply (PS2) at a common ground knot on the thruster.

Thruster performance could possibly change for either of two reasons: 1) energy was transferred electrostatically into the plasma, or 2) electric field lines were sufficiently altered by the applied field thereby causing a normal thruster discharge to be altered due to the presence of the external field.

The results of tests which examined possible performance changes due to electric field line changes are presented in Table 22. The experimental data shows that no effect on performance could be noted due to the presence of the external field applied by the insulated ring shaped electrode. Since the 0.5μfd capacitor was charged to a maximum of 3 KV, the maximum amount of energy that could possibly be transferred to the plasma of the main thruster discharge is thus only 2.25 joules. Since this amount of energy is very small compared to the energy of the main discharge, a second set of experiments were performed which examined the instantaneous voltage on the 0.5μfd capacitor. If energy is transmitted to the plasma one would expect the stored voltage on this capacitor to drop below its initial value. To reduce the self RC response time of the external field circuit, the capacitance was reduced to 0.05μfd.

A test was performed to verify that the externally applied field circuit is capable of releasing energy at a rate faster than the rate of energy released by the main thruster discharge. Figure 21 presents an oscilloscope trace of this test. The lower trace represents the voltage change across the conical electrode of the thruster during thruster operation of 3250 volts (385 joules). The total duration

TABLE 22. PERFORMANCE MEASUREMENTS WITH AND WITHOUT EXTERNALLY APPLIED ELECTROSTATIC FIELD

Log	Thruster Voltage (PS1) (volts)	External Field Voltage (PS2) (volts)	Ball Calibration (rel. units)	Thruster Deflect (rel. units)	Thruster Energy (joules)
153	2000	0	19.75	7.25	132.2
	2000	1450	19.75	7.25	132.2
154	3000	0	19	20.5	297.45
	3000	500	19	20	297.45
	3000	1000	19	20	297.45
	3000	1600	19	20	297.45
	3000	0	20	20.5	297.45
	3000	2000	20	20	297.45
	3000	2500	20	20	297.45
	3000	3000	20	20.5	297.45
	2000	0	20	8.5	132.2
	2000	3000	20	8.5	132.2
155	4000	0	20	35	528
	4000	500	20	35.5	528
	4000	1000	20	35.5	528
	4000	1500	20	35	528
	4000	2000	20	35	528
156	3250	0	18	21.5	358
	3250	500	18	21.7	358
	3250	1000	18	21.25	358
	3250	1500	18	21	358
	3250	2000	18	21	358
	3250	2500	18	21	358
	3250	3000	18	21	358

of the thruster discharge is about 7.5 sec. The largest voltage variation occurs during the first 3 microseconds. The upper trace shows the voltage variation across the 0.05μfd capacitor which is applying -2000 volts on the insulated electrode relative to the cathode of the thruster. The vacuum switch of the external field circuit was externally triggered to discharge its stored energy 0.55μsec after the main thruster discharge started. It is seen that the energy stored in the small capacitor was completely removed in about 1.75μsec with most of the energy removed within 1.0μ sec of this time. Thus the external field circuit was shown to be capable of releasing its energy in a time faster than 1.75 μsec (the 1.75 μsec discharge time included the total persistance of the arc in the vacuum switch). It was also verified that the external field circuit could be discharged at any preselected time relative to the main thruster discharge. This latter feature was achieved by using a single command pulse to fire the main thruster and by also feeding it through a controllable delay line before it activated the discharge initiating circuit of the igniter plug in the vacuum switch.

Subsequent studies with this circuitry led to the conclusion that no measureable transfer of energy occurred between the externally applied field and the plasma of the thruster.

Top Trace: Switch Voltage: 2000 volts/cm

Lower Trace: Thruster Voltage: 2000 volts/cm

Sweep Speed: 2 microsec/cm

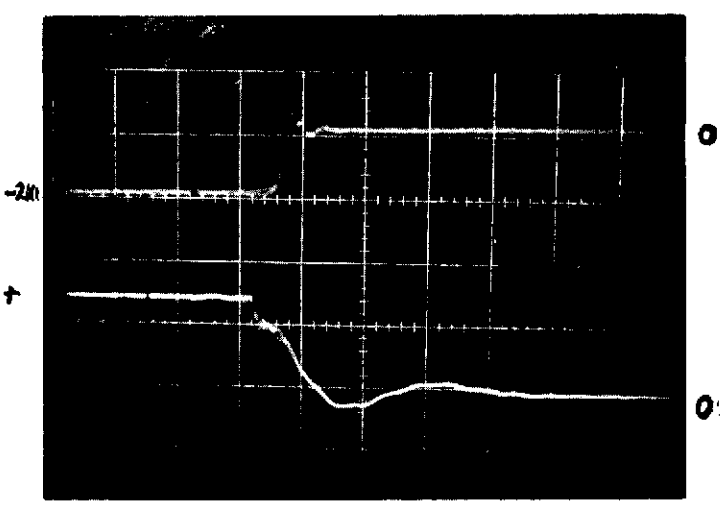

Figure 21. Discharge Behavior of External Field Circuit and Main Thruster Discharges

4.5 CONCLUDING REMARKS

The three separate studies examining the effect of the electrostatic field on thruster performance revealed that no noticeable effect in performance could be detected. It was found, however, that the ability to initiate a thruster discharge by solid state igniter plugs was strongly effected by the direction of the applied electrostatic field. Compared to either breech-fed or side-fed propellant thrusters, the conically shaped nozzle did produce a significantly higher thrust/power ratio at a given discharge energy level than had ever been measured with either of the two other geometries.

Because Burkhardt's comprehensive studies with a steady state plasma accelerator revealed a definite effect of the field on performance, his results were reexamined. A careful examination of his data showed that his downstream cathode thruster configuration produced a significantly better performance only when the specific impulse was in excess of about 1000 seconds. Since the measured specific impulse in the present study was only in the range of 500 to 600 seconds it is now realized that perhaps the results obtained must be considered inconclusive. The acceleration process encountered was most likely more gasdynamic in origin and electrostatic effects would not be expected to have a measureable effect on performance. Since this latter interpretation was reached only after completion of the experimental studies, it was not possible to repeat the studies at a higher specific impulse where electric field effects, as in Burkhardt's study, would be expected to be effective. Since the specific impulse of both breech-fed and side-fed thruster geometries can be changed by varying the ratio of discharge energy/propellant area it is expected that the same would be true of the conical configuration. In order to raise the specific impulse well above 1000 seconds, it would be necessary to increase the discharge energy/propellant area ratio. As with the other nozzle configurations, a limited number of parametric studies would have to be performed to establish the scaling relationship between this latter parameter and specific impulse. Due to program constraints such studies could not be implemented. Until such latter studies are carried out and the studies reported upon are repeated at a specific impulse considerably in excess of 1000 seconds it is believed that no definite conclusion can be made regarding the ability to augment pulsed plasma thruster performance by electrostatic field effects.

REFERENCES

1. Guman, W. J., "Quasi-Steady and Short Pulse Discharge Thruster Experiments," NASA CR-111935 Final Technical Report, PCD-TR-71-3, FHR 3795-1, PC004R7001, Fairchild Industries, Farmingdale, N.Y., June 1971. Also see AIAA paper 72-459, AIAA 9th Electric Propulsion Conference, Bethesda, Maryland, April 1972.

2. Palumbo, D. J., Guman, W. J., "Propellant Side-Feed Short Pulse Discharge Thruster Studies," NASA CR-112035, PCD-TR-72-1, FHR4031A, PC0049R9401, Fairchild Industries, Inc., Farmingdale, N.Y., Jan. 1972.

3. Palumbo, D. J., Guman, W. J., "Pulsed Plasma Propulsion Technology Report," AFRPL-TR-73-79, Air Force Rocket Propulsion Laboratory, Edwards AFB, California, September 1973.

4. Guman, W. J., Vondra, R. J., Thomassen, K., "Pulsed Plasma Propulsion System Studies," AIAA Paper 70-1148, AIAA 8th Electric Propulsion Conference, Stanford, California, September 1970.

5. Holcomb, L. B., "Survey of Satellite Auxiliary Electric Propulsion Systems," J. Spacecraft and Rockets, Volume 9, No. 3, March 1972, page 144.

6. Solbes, A., "Personal Communication," 12/2/71, Massachusetts Institute of Technology, Cambridge, Massachusetts, Department of Aeronautics and Astronautics.

7. Popov, N. P., Vereshchagin, V.L., "Study of the Erosion of a Dielectric in a Conical Plasma Accelerator," Samoletostroenie i Tekhnika Vozdushnogo Floto, No. 20, 1970. Available as AIAA-A-71-14597.

8. Khizhnyak, N. A., Safronov, B.G., Vereshchagin, V. L., "Electrodynamic Acceleration of a Plasma in a Conical Electrode Source," Soviet Physics-Technical Physics, Volume 13, No. 1, July 1968.

9. Khizhnyak, N. A., Safronov, B. G., Vereshchazin, V. L., Popov, N. P., "Electrode Erosion in Pulsed Plasma Accelerators," Soviet Physics - Technical Physics, Volume 15, No. 11, May 1971.

10. Azizov, E. A., Komelkov, V. S., Stepanenko, M. M., "Plasma-Jet Generator with Noncylindrical Electrode Geometry," Soviet Physics - Technical Physics, Volume 17, No. 1, July 1972.

11. Guzhovskii, I. T., Gaidukov, V. F., Belan, N. V., "Conical Electrode Source," Soviet Physics - Technical Physics, Volume 12, No. 7, January 1968.

12. Azouskii, Yu. S., Guzhovskii, I. T., Satronov, B. A., Churaev, V. A., "Conical Plasma Source," Soviet Physics - Technical Physics, Volume 7, No. 9, March 1963.

13. Burkhart, J. A., "Initial Performance Data on a Low Power Arc Thruster with a Downstream Cathode," AIAA Paper 70-1084, AIAA 8th Electric Propulsion Conference, Stanford, California, September 1970.

14. Burkhart, J. A., Seikel, G.R., "Feasibility Studies of an Auxiliary Propulsion System Using MPD Thrusters," AIAA Paper 71-695, AIAA SAE 7th Propulsion Joint Specialist Conference, Salt Lake City, Utah, June 1971.